의학박사 학위논문

AKR1C2 promotes metastasis and regulates the molecular features of luminal androgen receptor subtype in triple negative breast cancer cells

2023년 2월

서울대학교 대학원
협동과정 종양생물학전공
LI SONGBIN

Ph.D. Dissertation of Medicine

AKR1C2 promotes metastasis and regulates the molecular features of luminal androgen receptor subtype in triple negative breast cancer cells

삼중 음성 유방암에서 AKR1C2 유전자의 기능 연구

February 2023

Graduate School
Seoul National University College of Medicine
Interdisciplinary Program in Cancer Biology

LI SONGBIN

AKR1C2 promotes metastasis and regulates the molecular features of luminal androgen receptor subtype in triple negative breast cancer cells

지도교수 문 형 곤

이 논문을 의학박사 학위논문으로 제출함
2022년 10월

서울대학교 대학원
협동과정 종양생물학전공
LI SONGBIN

LI SONGBIN의 박사 학위논문을 인준함
2023년 1월

위 원 장 _____ (인)
부 위 원 장 _____ (인)
위 원 _____ (인)
위 원 _____ (인)
위 원 _____ (인)

AKR1C2 promotes metastasis and regulates the molecular features of luminal androgen receptor subtype in triple negative breast cancer cells

Advisor Hyeong-Gon Moon

Submitting a Ph.D. Dissertation of Medicine

October 2022

Graduate School
Seoul National University College of Medicine
Interdisciplinary Program in Cancer Biology

Songbin Li

Confirming the Ph.D. Dissertation written by Songbin Li
January 2023

Chair _____(Seal)
Vice Chair _____(Seal)
Examiner _____(Seal)
Examiner _____(Seal)
Examiner _____(Seal)

Abstract

AKR1C2 promotes metastasis and regulates the molecular features of luminal androgen receptor subtype in triple negative breast cancer cells

LI SONGBIN

Interdisciplinary Program in Cancer Biology

The Graduate School

Seoul National University

Patients with triple-negative breast cancer (TNBC) have an increased risk of distant metastasis compared to those with other subtypes. In this study, I aimed to identify the genes

associated with distant metastasis in TNBC and their underlying mechanisms. I established patient-derived xenograft (PDX) modelsusing surgically resected breast cancer tissues from 31 patientswith TNBC. Among these, 15 patients subsequently developed distant metastases. Candidate metastasis-associated genes were identified using RNA sequencing. *In vitro* wound healing, proliferation, migration, and invasion assays and *in vivo*tumor xenograft and metastasis assays were performed to determine the functional importance of aldo-keto reductase family 1 member C2 (AKR1C2). Additionally, I used the METABRIC dataset to investigate the potential role of AKR1C2 in regulating TNBC subtypes and their downstream signaling activities. RNA sequencing of primary and PDX tumors showed that genes involved in steroid hormone biosynthesis, including AKR1C2, were significantly upregulated in patients who subsequently developed metastasis. *In vitro* and *in vivo* assays showed that silencing of AKR1C2 resulted in reduced cell proliferation, migration, invasion, tumor growth, and incidence of lung metastasis. AKR1C2 was upregulated in the luminal androgen receptor (LAR) subtype of TNBC in the METABRIC dataset, and AKR1C2 silencing resulted in the downregulation of LAR classifier genes in TNBC cell lines. The androgen receptor (AR) gene was a downstream mediator of AKR1C2-associated

phenotypes in TNBC cells. AKR1C2 expression was associated with gene expression pathways that regulate AR expression, including JAK-STAT signaling or interleukin 6 (IL-6). The levels of phospho-signal transducer and activator of transcription 3 (p-STAT3) and IL-6, along with secreted IL-6, were significantly downregulated in AKR1C2-silenced TNBC cells. My data indicate that AKR1C2 is an important regulator of cancer growth and metastasis in TNBC and may be a critical determinant of LAR subtype features.

Keywords: Aldo-Keto Reductase Family 1 Member C2; Neoplasm Metastasis; Receptors, Androgen; Triple Negative Breast Neoplasms

Student Number: 2020-39163

Part of this thesis research has been accepted for publication in Journal of Breast Cancer.

Table of Contents

List of Tables

List of Figures

List of Abbreviations

TNBC: Triple negative breast cancer

PDX: Patient derived xenograft

AKR1C2: Aldo-keto reductase family 1 member C2

LAR: Luminal androgen receptor

AR: Androgen receptor

IL-6: Interleukin 6

p-STAT3: Phospho-signal transducer and activator of transcription 3

ER: Estrogen receptor

PR: Progesterone receptor

HER2: Human epidermal growth factor receptor 2

BL1: Basal like 1

BL2: Basal like 2

IM: Immunomodulatory

M: Mesenchymal

MSL: Mesenchymal stem-likeUNS: Unspecified

group.

RFS: Relapse free survival

DMFS: Distant metastasis-free survival

OS: Overall survival

DFS: Disease free survival

siRNA: Small interfering RNA

shRNA: Short hairpin RNA

PCR: Real-time polymerase chain reaction

mRNA: Messenger RNA

H&E staining: Hematoxylin and eosin staining

ELISA: Enzyme-linked immunosorbent assay

CTL: Control

SD: Standard deviation

FC: Fold change

KEGG pathway: Kyoto Encyclopedia of Genes and Genomes

ns: Not significant

I. Introduction

Breast cancer is the most common malignancy in women worldwide [1]. It is also the most common malignancy in women in Korea, and its incidence has been increasing during the last few decades [2, 3]. Although most breast cancers can be effectively treated with current multimodal treatment options, a substantial number of patients eventually develop distant metastasis and die [4].

Triple-negative breast cancer (TNBC) accounts for 10-20% of all breast cancers and is characterized by a lack of estrogen receptor (ER), progesterone receptor (PR), and human epidermal growth factor receptor 2 (HER2) expression. Compared with other subtypes of breast cancer, TNBC has a shorter time to metastasis and recurrence, has fewer treatment options, and is more likely to metastasize to visceral organs such as the lung or liver [5-7]. Therefore, there are ongoing efforts to better understand the molecular mechanisms underlying TNBC.

The patient-derived xenograft (PDX) model is a preclinical research model established by transplanting patient tumor tissue into immunodeficient mice. While some studies have suggested potential limitations of the PDX model in terms of maintaining the

biological fidelity of the primary tumors [8, 9], many studies have shown that the genetics, gene expression patterns, and histology of PDX tumors are generally stable and can effectively recapitulate the patient' s tumor characteristics [10-15]. PDX models can also preserve tumor characteristics, such as cell-cell interactions within the tumor microenvironment, and may provide insights into the mechanisms of drug resistance in cancer [16-18]. Importantly, PDX models of patients with breast cancer have been shown to accurately predict the clinical outcomes of donor patients, suggesting that these models can be effectively used to provide biological insights into the processes of distant metastasis [15, 19].

The overall prognosis of TNBC patients is poor [5], and they are not sensitive to endocrine therapy and targeted therapy. To develop new therapies, a better understanding of the molecular mechanisms of TNBC is needed. In 2011, Lehmann et al. [20] divided TNBC into BL1, BL2, IM, M, MSL and LAR subtypes according to the gene expression of TNBC patients. And these subtypes exhibit different prognosis in TNBC. In TNBC, targeted therapies based on the gene expression signatures of these subtypes may achieve better efficacy. The representative gene in the LAR subtype is AR [20]. However, the role of AR in TNBC has been controversial. Some studies have shown that AR

can lead to poor prognosis in TNBC [20, 21], while some have shown the opposite result [22, 23]. I compiled 21 studies on the involvement of AR in the prognosis of TNBC patients, as shown in Table 1. The research on AR mainly focuses on prostate cancer. In most prostate cancer-related studies, the activation of AR signaling can promote tumor progression [24]. AR also plays an important role in breast cancer. Studies have shown that AR can promote the proliferation of breast epithelial cells and the expansion of ducts in breast cancer [25, 26], especially in TNBC, AR can promote tumor cell proliferation by activating MAPK/ERK signaling [27]. In the present study, I investigated the role of AR in TNBC based on analysis of public databases and in vitro experiments.

Table 1. AR in TNBC has different clinical outcomes

Reference	Dataset	No. of TNBC patients	Good prognosis	Poor prognosis	No significant	Note
Lehmann, et al. 2011 [20]	GSE4394, GSE7904, GSE2109, GSE7390, GSE2990, GSE1456, GSE22513, GSE28796, GSE11121, GSE2603, GSE5364, GSE1561, GSE5327, GSE5847, GSE12276, GSE16446, GSE18864, GSE19615, GSE20194, MDA1333 and ETABM158	n=587		O (RFS)		Poor RFS may be related to the generally higher age of patients with LAR subtype.
Sutton, et al. 2012 [22]	clinical data	n=121	O (DMFS)			AR is negatively correlated with Ki-67

Thike, et al. 2014 [23]	clinical data	n=699	O (OS)			Reduced androgen receptor signaling encourages neoplastic transformation in mammary epithelial cells harboring BRCA1 mutations
Pistelli, et al. 2014 [28]	clinical data	n=81			O	
McGhan, et al. 2014 [29]	clinical data	n=94			O	
Gasparini, et al. 2014 [30]	clinical data	n=153	O (OS)			AR is negatively correlated with CDK6
Burstein, et al. 2015 [31]	clinical data	n=198		O (DFS)		The CCND1 and FGFR2 genes are amplified in LAR tumors
Choi, et al. 2015 [32]	clinical data	n=87		O (OS, DFS)		AR upregulates the expression of MMP-9 and COX-2
Ricciardi, et al. 2015 [33]	clinical data	n=45	O (OS)			AR is negatively correlated with Ki-67
Lehmann, et al. 2016 [21]	GSE4394, GSE7904, GSE2109, GSE7390, GSE2990, GSE1456, GSE22513, GSE28796, GSE11121, GSE2603, GSE5364, GSE1561, GSE5327, GSE5847, GSE12276, GSE16446, GSE18864, GSE19615, GSE20194, MDA1333 and ETABM158, TCGA	n=767		O (OS, DMFS)		Prognosis may be related to age and chemosensitivity
Asano, et al. 2016 [34]	clinical data	n=61		O (RFS)		AR inhibits the expression of E-cadherin
Yuka Asano, et al. 2017 [35]	clinical data	n=190	O (RFS)			It may be related to the effect of AR on the expression of FOXA1.
Hu, et al. 2017 [36]	clinical data	n=360	O (OS, DFS)			AR is negatively correlated with CK5/6
Bareche, et al. 2018[37]	METABRIC, TCGA	n=550		O (OS)		The LAR subtype shows the worst prognosis

Astvatsaturyan, et al. 2018[38]	clinical data	n=135			O	
Sunar, et al. 2018 [39]	clinical data	n=84			O	
Dieci, et al. 2019 [40]	clinical data	n=263		O (DDFS)		AR is positively correlated with FOXA1
Anita Mangia, et al. 2019 [41]	clinical data	n=124		O (DFS)		AR affects tumor infiltrating lymphocytes and FOXA1
Bhattarai, et al. 2019 [42]	clinical data	n=1407			O	
Govindan, et al. 2020 [43]	clinical data	n=101		O (DMFS)		AR is positively correlated with FOXA1 and GATA3
Lyalkin, et al. 2020 [44]	clinical data	n=116	O (OS)			The role of AR is not described.

In this study, by performing RNA sequencing using primary tumors and their corresponding PDX tumors, I identified a metastasis-related gene, aldo-keto reductase family 1 member C2 (AKR1C2), in breast cancer. Additionally, my data demonstrate that AKR1C2 regulates androgen receptor (AR) expression and modulates the features of the luminal androgen receptor (LAR) subtype in TNBC.

II. Materials and Method

Breast cancer cell lines and small interfering RNA (siRNA) treatment

Breast cancer celllines were purchased from the Korean Cell Line Bank (Seoul, Korea). MDA-MB-231 and MDA-MB-468 cells were obtained from the American Type Culture Collection (Manassas, VA, USA) and were cultured in Dulbecco's Modified Eagle's medium (Biowest LLC, Riverside, MO, USA) supplemented with 10% fetal bovine serum (FBS; Gibco, Waltham, MA, USA) and 1% penicillin/streptomycin (Gibco). Commercially available AR (gene ID: 367), AKR1C1 (gene ID: 1645), AKR1C3 (gene ID: 8644), and AKR1C4 (gene ID:1109) siRNAs were purchased from Bioneer (Daejeon, Korea). The cells were seeded 1 × 10^6cells/well in 6-well plates. After the cells were attached, I diluted Lipofectamine-RNAi MAX Reagent (Invitrogen, Waltham, MA, USA) and siRNA 10 nM (Dharmacon, Lafayette, CO, USA) in Opti-MEM. After incubation for 5 minutes, I treated Lipofectamine and siRNA mixture to attached cells and incubated for 2 days at 37° C. Next, I analyzed the

transfected cells.

Cell transfection

The pLKO.1-Puro lentiviral vector was constructed to contain sequences of specific short hairpin RNA (shRNA) targeting human AKR1C2 (pLKO.1-AKR1C2-shRNA: Forward: CCGGACAGGCTGCTGGAGATGATCCCTCGAGGGATCATCTCCAGCAGCCTGTTTTTTG, Reverse: AATTCAAAAAACAGGCTGCTGGAGATGATCCCTCGAGGGATCATCTCCAGCAGCCTGT). Constructs containing pLKO.1-AKR1C2-shRNA were transfected into HEK-293FT cells using Lipofectamine 3000 (Thermo Fisher Scientific, Waltham, MA, USA). After incubation in a CO_2 incubator at37° C for 48 hours after transfection, the medium containing lentivirus was harvested and used for infecting MDA-MB-231 and MDA-MB-468. Cells with pLKO.1-Puro scramble shRNA (shCTL) were used as negative controls.

Proliferation assay

Cells were plated in flat-bottom 96-well culture plates (1×10^4cellsperwell). The cells were incubated with 0.5mg/mL thiazolyl blue tetrazolium bromide (MTT; Sigma-Aldrich, St. Louis, MO, USA) for 4 hours at 37° C. The medium was discarded, and 200 μL of dimethyl sulfoxide (Duchefa Biochemie, Haarlem, The Netherlands) was added to each well to dissolve the formazan crystals in the cells. The absorbance was measured at 570 nm using a microplate reader (BioTek Instruments, Winooski, VT, USA).

Cell invasion, migration, and wound healing assay

In the invasion assay, 1 mg/mL Matrigel was added to the insert before seeding the cells, but this was not the case in the migration assay. Medium supplemented with 10% FBS was added to the lower chambers. Cells were incubated for 24 hours, fixed with 4% paraformaldehyde (Biosesang, Seoul, Korea), and stained with 0.1% crystal violet (Sigma-Aldrich). Quantitative evaluation of the migrated and invaded cells was performed using the ImageJ (Java 1.8.0_172) software (NIH, Bethesda, MD, USA).

For the wound healing assay, the cell lines were seeded in

6-well plates. Monolayers were scraped with a pipette tip after 24 hours incubation in a serum-free medium and washed with a serum-free medium to remove floating cells. The cells were photographed every 12 hours at two randomly selected sites per well.

Western blotting

Cell lysates were harvested using radioimmunoprecipitation assay buffer (Thermo Fisher Scientific), protease, and phosphatase inhibitor (Thermo Fisher Scientific), incubated for 10 minutes on ice, and centrifuged at 14,000 rpm for 15 minutes at 4° C. The protein concentration was measured using a bicinchoninic acid assay kit (Thermo Fisher Scientific), separated by sodium dodecyl sulfate-polyacrylamide gel electrophoresis, and transferred to polyvinylidene fluoride (Sigma-Aldrich) membranes. After blocking with 5% bovine serum albumin (Biosesang, Seoul, Korea) solution, membranes were incubated with primary antibody overnight at 4° C. The secondary antibody was diluted (1:10,000) in a 5% skim milk solution. Western blotting bands were detected using an Amersham Imager 680 (GE Healthcare Life Sciences, Chicago, IL, USA). The following

antibodies were used: β-actin (#sc-47778; Santa Cruz Biotechnology, Dallas, TX, USA), AKR1C2 (#13035; Cell Signaling Technology, Danvers, MA, USA), AR (#5153; Cell Signaling Technology), signal transducer and activator of transcription 3 (STAT3, #9139; Cell Signaling Technology), phosphorylated STAT3 (pSTAT3, #9138; Cell Signaling Technology), and interleukin 6 (IL-6, #12153; Cell Signaling Technology).

Real-time polymerase chain reaction (PCR)

Total RNA was extracted from the cells using TRIzol Reagent (Favorgen, Ping-Tung, Taiwan). The Prime Script 1st strand cDNA Synthesis Kit (Takara, Osaka, Japan) was used for reverse transcription of RNA, and qPCR assays were performed using Power SYBR Green PCR Master mix (Thermo Fisher Scientific). The reactions were performed using an ABI7500 real-time PCR System (Thermo Fisher Scientific). To compare relative messenger RNA (mRNA) expression levels, gene expression levels were expressed as ratios relative to glyceraldehyde 3-phosphate dehydrogenase. Primer sequences are shown in Table 2.

Table 2. Information on used primer sequences

Gene	Orientation	Primer Sequence (5'−3')
AKR1C1	Forward	TGTCCAACTTCAACCGCAGG
	Reverse	CCCATGGTTCTTCTCGGTGG
AKR1C2	Forward	CAACTTCAACCACAGGCTGC
	Reverse	GGGTCCACCCATGGTTCTTC
AKR1C3	Forward	GGGTGTCAAACTTCAACCGC
	Reverse	GGTCCACCCATCGTTTGTCT
AKR1C4	Forward	TCGGGGTGTCAAACTTCAACT
	Reverse	ACCCATAGTTTATGTCGTTGGG
hGAPDH	Forward	ACCCAGAAGACTGTGGATGG
	Reverse	TTTCTAGACGGCAGGTCAGG
DHCR24	Forward	TGCCTCCCAAGATCTCCCTC
	Reverse	TGTCGTTTTGGAAGGTGTGC
APOD	Forward	ACAACCTTTGAGAATGGACGC
	Reverse	GGTGGCTTCACCTTCGATTTG
PIP	Forward	ACGTCCAAATGACGAAGTCAC
	Reverse	CGTCACATAGGCAGGCAGTAT
ALCAM	Forward	AACACGATGAGGCAGACGAG
	Reverse	CAGCCAGTAGACGACACCAG
AR	Forward	(Product name: P171456) Primers were purchased from Bioneer (South Korea)
	Reverse	
AURKB	Forward	GGGAACCCACCCTTTGAGAG
	Reverse	GGGGTTATGCCTGAGCAGTT
CENPF	Forward	TGCCTCTTTGCAGGACACAT
	Reverse	TGCAGCTCAGTTTCCTTTGC
BUB1	Forward	TTATCTGCTGGCTTGGCACT
	Reverse	TCGATCTGGTAGTTCCATGGTT
FANCG	Forward	GCCCAGGTAATCGAGACACT
	Reverse	CCTTAGTTTGGGCCTCCAGC
MCM2	Forward	GGCGTGACAACAATGAGCTG
	Reverse	CCAAGTCCTTCTCAGGGACC

Hematoxylin and eosin (H&E) staining

Tissues were fixed in 4% para-form aldehyde for 48 hours. After processing, the processed tissues were embedded in paraffin blocks. To identify the histological structure, paraffin blocks were sectioned to a thickness of approximately 4 ㎛ using a microtome. After drying the section slides, paraffin was removed from the sections using xylene, followed by dehydration with ethanol. After dehydration, the nuclei were stained with hematoxylin solution and cytosol with eosin, according to the manufacturer's protocol.

IL-6 enzyme-linked immunosorbent assay (ELISA)

Measurements were performed on the conditioned medium of transfected MDA-MB-231 cells using a Human IL-6 Human ELISA Kit (#EH2IL6; Thermo Fisher Scientific). The conditioned medium was diluted with diluent buffer and added to each well. After incubating for 3 hours at 4° C, each well was washed and incubated for 1 hour at 4° C with human IL-6 conjugate. After

washing, substrate solution was added to each well, followed by incubation for 30 minutes. With stop solution addition, each well was read by a microplate reader, followed by calculation of IL-6 concentration with an optical density at 450 nm wavelength.

Established PDX and xenograft murine model

Breast cancer tissues were obtained from surgical specimens obtained during curative or palliative surgery. The acquisition of tissue and clinical and pathologic data from patients with breast cancer for this study was approved by the Institutional Review Board of Seoul National University Hospital(No. H-1707-174-874). Six-week-old female mice were used for the *in vivo*experiments. All experiments involving mouse models were approved by the Institutional Animal Care and Use Committee of the Seoul National University Hospital(No. 19-0096-S1A1, 22-0146-S1A0), and animals were maintained in the facility accredited by AAALAC International (#001169) in accordance with the Guide for the Care and Use of Laboratory Animals 8th edition, NRC (2010).

To establish the PDX model, surgically excised tissue was cut into small pieces of approximately 2mm and transplanted into

NOD/solid IL2Rg mouse mammary fat pads. After the tumor volume reached 1,000 mm^3, surgical resection was performed, and the tumor tissue was subjected to transcriptome analysis. To establish a xenograft model, MDA-MB-231 cells stably transfected with shCTL and shAKR1C2 were injected into the fat pads of 6-week-old athymic female nude mice (1×10^6cells/mouse). There were five mice each in the control and experimental groups. The length and width of each tumor were measured using calipers, and the volume was calculated using the following equation: $V = (\text{length} \times \text{width}^2)/2$. Tumor volume was measured twice a week until the tumor size reached 1,000 mm^3,after which surgical resection was performed. The mice were sacrificed 4 weeks after the operation and lung metastases were observed. MDA-MB-231 cells stably transfected with shCTL or shAKR1C2 were injected into the tail vein of 6-week-old mice (5×10^5 cells/mouse). There were five mice eachin the control and experimental groups. Mice were sacrificed after four weeks, and lung tumor metastasis was observed.

RNA sequencing and bioinformatics

RNA sequencing libraries were prepared using the TruSeq

Stranded mRNA Prep kit (Illumina, Inc., San Diego, CA, USA), according to the manufacturer' s protocol. Paired-end 101 bp RNA sequencing was performed using a Novaseq 6000 system (Illumina, Inc.). Sequenced RNA reads were aligned to a chimeric reference genome (human hg38 and mouse mm10) using the RSEM-1.3.1. To normalize gene expression levels, I separated raw read counts by the organism and normalized the counts to FPKM using htseq-count. Differentially expressed genes (DEGs) were called using edgeR-3.30.3 for each comparison group.

Statistical analysis

GraphPad Prism ver. 8 (GraphPad Software, San Diego, CA, USA) was to generate graphs and perform statistical tests. Data values are presented as mean±standard deviation (SD), and Mann-Whitney *U* tests were used to compare the means between the groups. For the size of tumor volumes, I used two-way analysis of variance (ANOVA) for comparison. Spearman correlation analysis was used to verify the correlation between genes. Survival curves were constructed using the Kaplan-Meier method and compared between TNBC subtypes

with the log-rank test. Survival analyses were performed using SPSS 26 (IBM Corp., Armonk, NY, USA).

III. Results

Gene expression signatures of primary tumors and PDX tumors in patients with TNBC with distant metastases.

I established TNBC PDX models using tumor tissues obtained during breast surgery from 31 patients with breast cancer. Subsequently, 15 patients (48.4%) developed distant metastasis during the follow-up period and the remaining 16 patients were disease-free (Table 3). Since the cells within the tumor microenvironment are replaced by murine stromal cells in PDX tumors, RNA sequencing of PDX tumors can generate gene expression data that are more enriched with epithelial cancer cells by excluding murine sequencing reads [45, 46]. Therefore, I hypothesized that incorporating the RNA sequence reads of both PDX tumors and corresponding primary tumors could enrich metastasis-related genes originating from epithelial cancer cells. I obtained 18 corresponding primary tumor tissues from 31 TNBC PDX models and identified 304 genes that were significantly upregulated in both PDX tumors and primary tumors

from patients who developed clinical distant metastasis (Figure 1).

Table 3. Patients' age, disease-free survival, and metastatic site

PDX_ID	Age	DFS(month)	Metastatic site	Subtype
X12	30	5	Liver, SCN, neck, bone	TNBC
X125	57	17	Lung	TNBC
X148	40	20	Local recur -> lung	TNBC
X257	32	11	Chest wall -> bone	TNBC
X61	38	3	Chest wall, liver	TNBC
MX_285	50	15	Liver	TNBC
MX_215	46	13	Lung, mediastinal LN	TNBC
MX_237	78	1	Lung	TNBC
MX_173	33	11	Lung, brain	TNBC
MX_197	55	1	Contralateral breast, Lung	TNBC
MX_258	47	8	Brain	TNBC
MX_276	52	9	Lung, mediastinal LN	TNBC
MX_347	35	9	Lung, bone	TNBC
MX_373	55	1	Pleura, lung	TNBC
MX_408	35	6	Lung, LN	TNBC
X134	27	63		TNBC
X141	54	73		TNBC
X142	61	72		TNBC
X192	38	89		TNBC
X196	56	88		TNBC
X27	62	94		TNBC
MX_130	51	86		TNBC
MX_158	65	89		TNBC
MX_195	51	85		TNBC
MX_214	51	83		TNBC
MX_227	72	81		TNBC
MX_231	58	84		TNBC
MX_247	33	79		TNBC
MX_308	77	46		TNBC
MX_363	56	73		TNBC
MX_404	27	63		TNBC

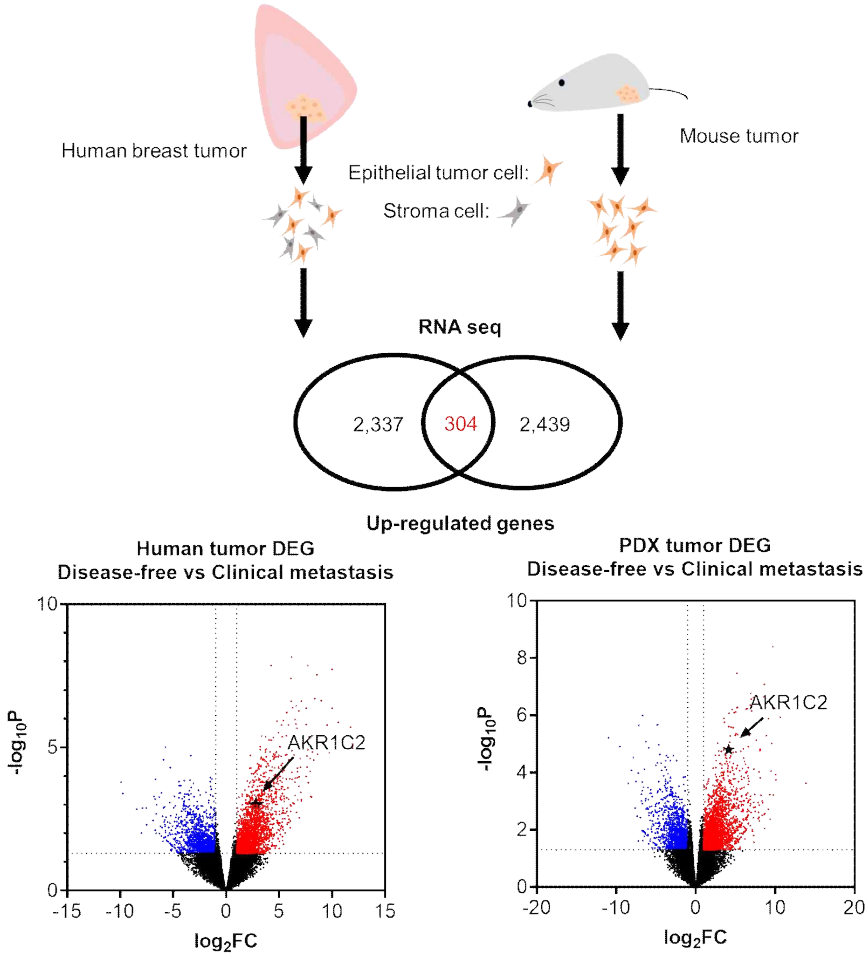

Figure 1. Schematic representation of human and PDX primary tumor RNA sequencing experiments. The Venn diagram shows upregulated genes in the tumors that developed distant metastasis, and the volcano plot illustrates the upregulation of AKR1C2.

KEGG pathway analysis (https://david.ncifcrf.gov/) was performed on these overlapping genes. patients who developed clinical distant metastasis (Figure 2A). Interestingly, 304 upregulated genes were enriched with genes involved in steroid hormone biosynthesis (Figure 2B, Table 4). Among the upregulated genes in steroid hormone biosynthesis, AKR1C2 showed the highest level of upregulation (Figure 2B, Table 5).

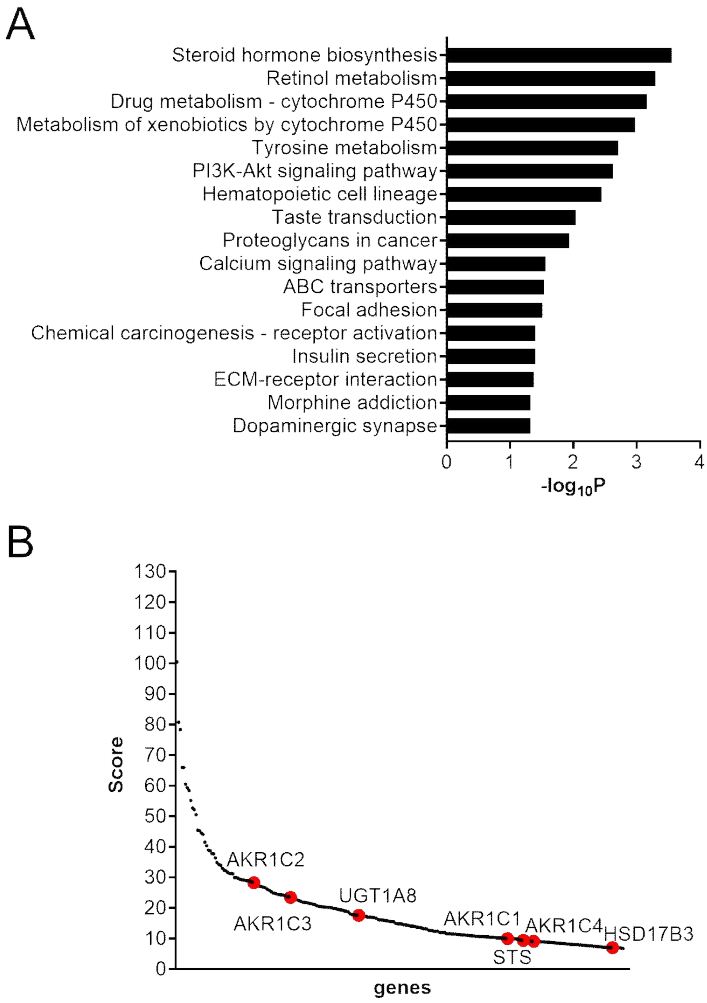

Figure 2. Identification of AKR1C2 as a potential gene regulating breast cancer metastasis. (A) KEGG pathways significantly enriched with the 304 genes that are upregulated in both patient' s tumor tissue and PDX tumor tissue. (B) The red dots indicate genes involved in the steroid hormone biosynthetic pathway.

Table 4. Pathway analysis of 304 upregulated genes

Term	Count	%	P-Value	Genes
Steroid hormone biosynthesis	7	2.39726	2.81E-04	*STS, AKR1C1, AKR1C3, HSD17B3, AKR1C2, AKR1C4, UGT1A8*
Retinol metabolism	7	2.39726	5.08E-04	*CYP2B6, RDH12, DHRS9, ADH1C, ADH1B, AOX1, UGT1A8*
Drug metabolism - cytochrome P450	7	2.39726	6.91E-04	*GSTM1, CYP2B6, ADH1C, ADH1B, AOX1, GSTT1, UGT1A8*
Metabolism of xenobiotics by cytochrome P450	7	2.39726	0.001057	*GSTM1, CYP2B6, ADH1C, ADH1B, AKR1C1, GSTT1, UGT1A8*
Tyrosine metabolism	5	1.712329	0.001939	*DCT, ADH1C, TH, ADH1B, AOX1*
PI3K-Akt signaling pathway	14	4.794521	0.002359	*CSF3, CSF3R, TNXB, HGF, TNC, IGF2, FGF2, EREG, FGF5, VTN, GNG2, CHAD, IL7R, FGF10*
Hematopoietic cell lineage	7	2.39726	0.003577	*IL1A, CSF3, CSF3R, CSF2, MME, IL7R, CD34*
Taste transduction	6	2.054795	0.009164	*PDE1B, GABRA3, HTR3A, HTR3B, PLCB1, SCN2A*
Proteoglycans in cancer	9	3.082192	0.011603	*VTN, CAV2, CAV1, HGF, IGF2, WNT7A, FLNC, FGF2, ANK1*
Calcium signaling pathway	9	3.082192	0.027217	*FGF5, CYSLTR1, EDNRB, CCKAR, PDE1B, HGF, PLCB1, FGF2, FGF10*
ABC transporters	4	1.369863	0.029378	*ABCD2, ABCB1, ABCC8, ABCC6*
Focal adhesion	8	2.739726	0.030858	*VTN, TNXB, CAV2, CAV1, HGF, CHAD, TNC, FLNC*
Chemical carcinogenesis - receptor activation	8	2.739726	0.039463	*FGF5, GSTM1, CYP2B6, CHRNA9, GSTT1, UGT1A8, FGF2, FGF10*
Insulin secretion	5	1.712329	0.039606	*ADCYAP1R1, CCKAR, ABCC8, ATP1A2, PLCB1*
ECM-receptor interaction	5	1.712329	0.042527	*VTN, TNXB, SV2A, CHAD, TNC*
Morphine addiction	5	1.712329	0.047131	*GNG2, PDE1B, PDE2A, GABRA3, PDE3A*
Dopaminergic synapse	6	2.054795	0.047601	*GRIA1, GNG2, TH, KIF5C, KIF5A, PLCB1*
Chemical carcinogenesis - reactive oxygen species	8	2.739726	0.049515	*GSTM1, HGF, AKR1C1, AKR1C3, AKR1C2, GSTT1, AKR1C4, COX7A1*

Table 5. AKR1C2 showed the highest upregulation of steroid hormone biosynthesis

Genes ranking	Human + PDX score	Human			PDX		
		logFC	q-value	Score	logFC	q-value	Score
AKR1C2	28.3088	2.79662	2.99683	8.38101	4.15689	4.79393	19.9278
AKR1C3	23.4647	2.40016	3.46055	8.30587	3.20286	4.7329	15.1588
UGT1A8	17.5964	3.24661	1.96276	6.37232	5.37107	2.08973	11.2241
AKR1C1	9.95868	2.154	2.32996	5.01874	2.05823	2.4001	4.93994
STS	9.40079	1.78779	3.50961	6.27443	1.50814	2.07298	3.12636
AKR1C4	9.09725	1.65444	1.5504	2.56505	2.40798	2.71274	6.53221
HSD17B3	7.00582	2.01713	1.63345	3.29487	2.20159	1.68558	3.71095

AKR1C2 promotes in vitro growth and migration of TNBC cells.

The AKR1C2 gene catalyzes nicotinamide adenine dinucleotide (NADH) and nicotinamide adenine dinucleotide phosphate (NADPH)-dependent conversion from dihydrotestosterone to 3α-diol [47, 48]. I examined the expression level of AKR1C2 in a panel of breast cancer cells. Breast cancer cells showed heterogeneous levels of AKR1C2 expression (Figure 3A). To verify whether the expression of AKR1C2 differs among breast cancer subtypes, the expression of AKR1C2 in 42 breast cancer cell lines was downloaded from the CCLE database for statistical analysis (https://sites.broadinstitute.org/ccle/). AKR1C2 was significantly upregulated in basal-like (BL) breast cancer cell lines in the CCLE database (Figure 3B).

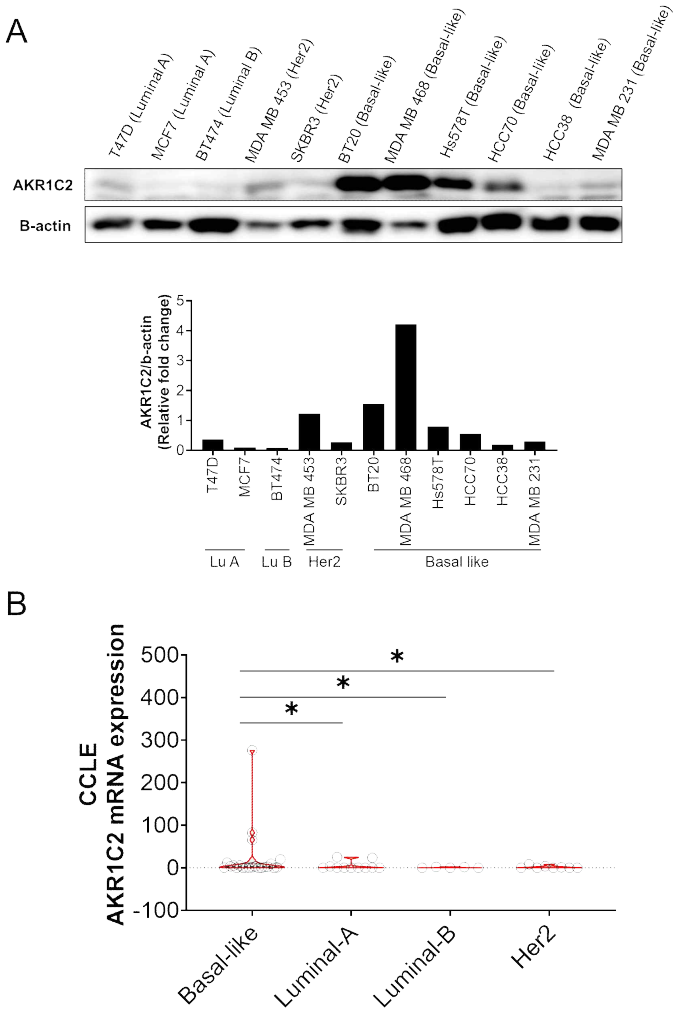

Figure 3. Expression of AKR1C2 in breast cancer cell lines. (A) The AKR1C2 protein expression levels in various breast cancer cell lines. **(B)** The AKR1C2 gene expression levels in breast cancer subtypes in the CCLE dataset. Error bars denote mean ± SD. $^{*}p \leq 0.05$. p-values were determined by the Mann-Whitney test.

To determine the functional significance of AKR1C2 in TNBC, I silenced AKR1C2 in MDA-MB-231 cells using shRNA against AKR1C2 (Figure 4A, B). Silencing of AKR1C2 significantly reduced the proliferation rate of breast cancer cells (Figure 5A, 5B). Wound healing and transwell cell migration assays showed that AKR1C2 silencing resulted in reduced cell migration (Figure 6A, 6B). Additionally, silencing AKR1C2 in MDA-MB-231 cells and MDA-MB-468 cells decreased Matrigel invasion capacity (Figure 7A, 7B). The results of these in vitro experiments suggested that AKR1C2 can regulated various aspects of breast cancer phenotypes by promoting cell growth and migration.

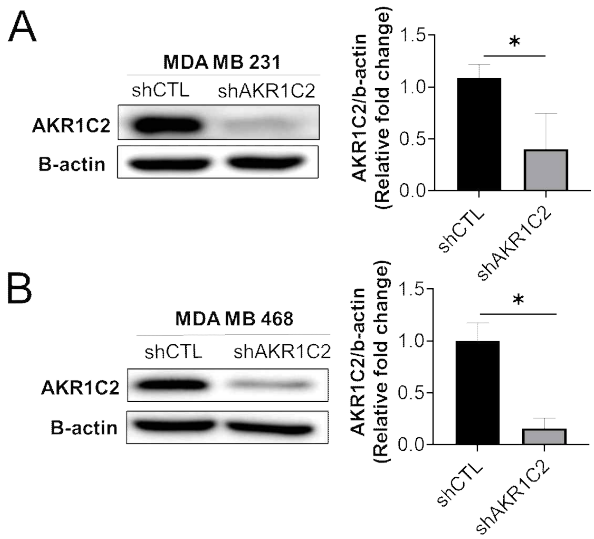

Figure 4. AKR1C2 protein expression levels in shAKR1C2-treated breast cancer cell lines. (A) AKR1C2 protein expression levels in shAKR1C2-treated MDA-MB-231 cells. **(B)** AKR1C2 protein expression levels in shAKR1C2-treated MDA-MB-468 cells. Error bars denote mean ± SD. $^{*}p \leq 0.05$. p-values were determined by the Mann-Whitney test.

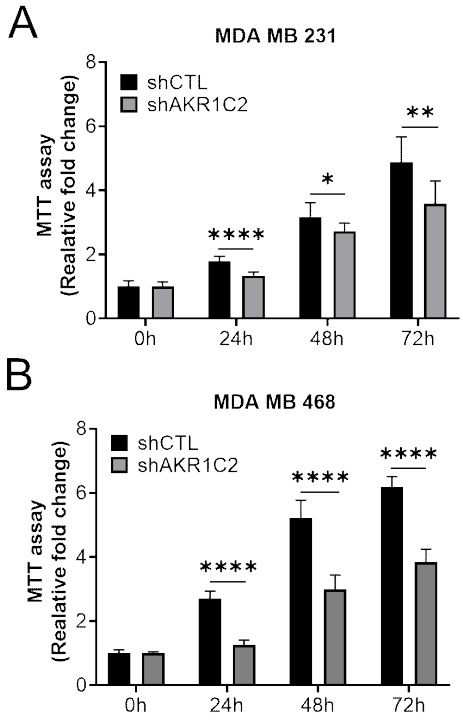

Figure 5. Viability of shAKR1C2-treated breast cancer cell lines. (A) Results of MTT assay using AKR1C2-silenced MDA-MB-231 cells. (B) Results of MTT assay using AKR1C2-silenced MDA-MB-468 cells. Error bars denote mean ± SD. $^{*}p \leq 0.05$, $^{**}p \leq 0.01$, $^{****}p \leq 0.0001$. p-values were determined by the Mann-Whitney test.

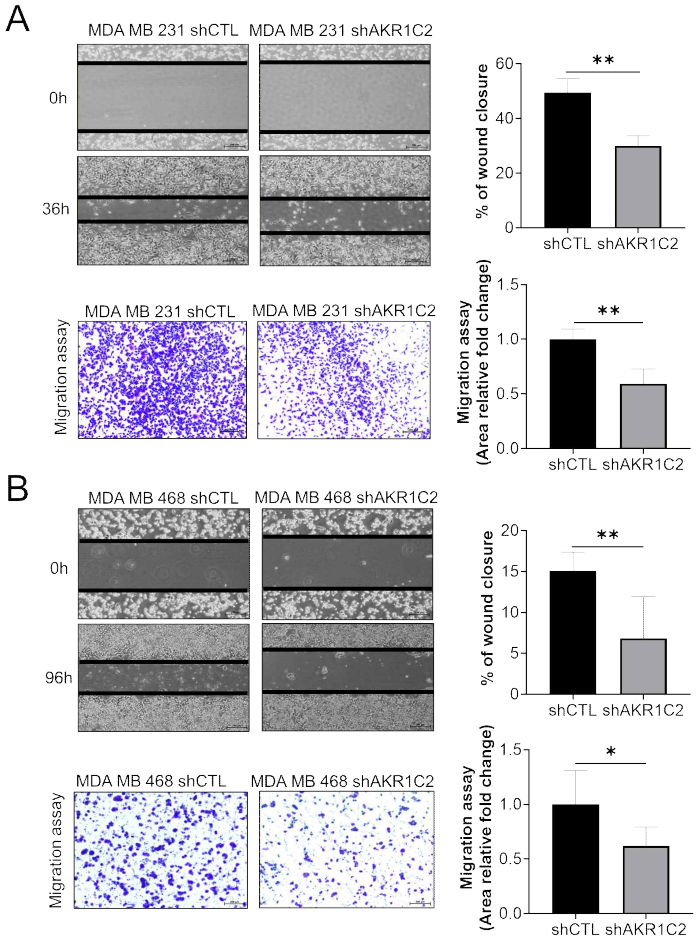

Figure 6. Mobility of shAKR1C2-treated breast cancer cell lines. **(A)** Representative images and quantitative results of wound healing assay, migration assay using AKR1C2-silenced MDA-MB-231 cells. **(B)** Representative images and quantitative results of wound healing assay, migration assay using AKR1C2-silenced MDA-MB-468 cells. Error bars denote mean ± SD. $^{*}p \leq 0.05$, $^{**}p \leq 0.01$. p-values were determined by the Mann-Whitney test.

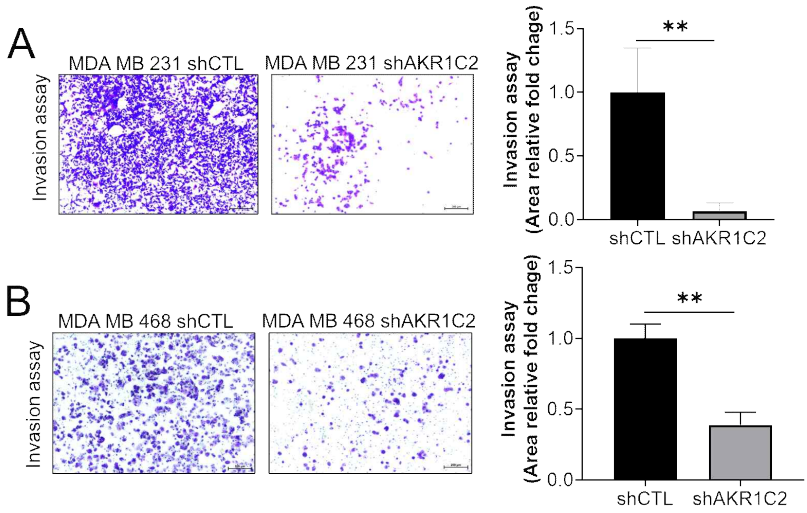

Figure 7. Invasive ability of shAKR1C2-treated breast cancer cell lines. (A) Representative images and quantitative results of invasion assay using AKR1C2-silenced MDA-MB-231 cells. **(B)** Representative images and quantitative results of invasion assay using AKR1C2-silenced MDA-MB-468 cells. Error bars denote mean ± SD. $^{**}p \leq 0.01$. p-values were determined by the Mann-Whitney test.

Effect of AKR1C family-related genes in breast cancer

I examined whether other genes in the aldo-keto reductase family exert similar effects on TNBC cells by silencing AKR1C1, AKR1C3, and AKR1C4 in TNBC cells (Figure 8). Silencing of these genes resulted ina modest reduction in cell proliferation and invasion (Figure9), but there was no significant effect on cell migration (Figure10). The results of these *in vitro* experiments suggest that AKR1C2 regulates various aspects of breast cancer phenotypes by promoting cell growth and migration in TNBC cells.

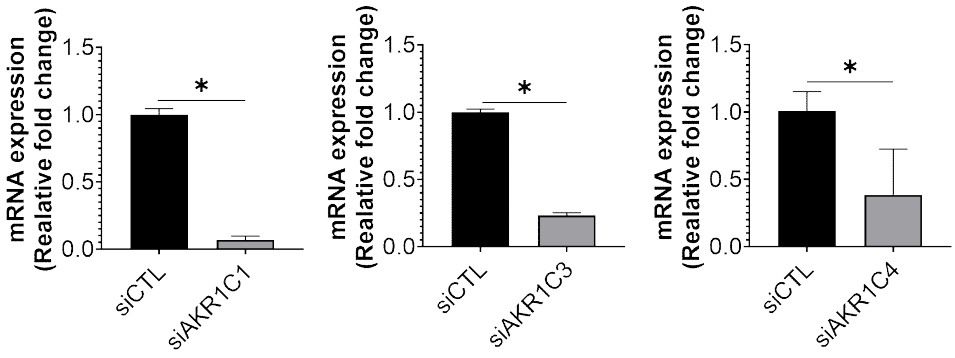

Figure 8. Gene expression levels of AKR1C1, AKR1C3, and AKR1C4 in MDA-MB-231 cells after using siRNA. Error bars denote mean ± SD. $^{*}p \leq 0.05$. p-values were determined by the Mann-Whitney test.

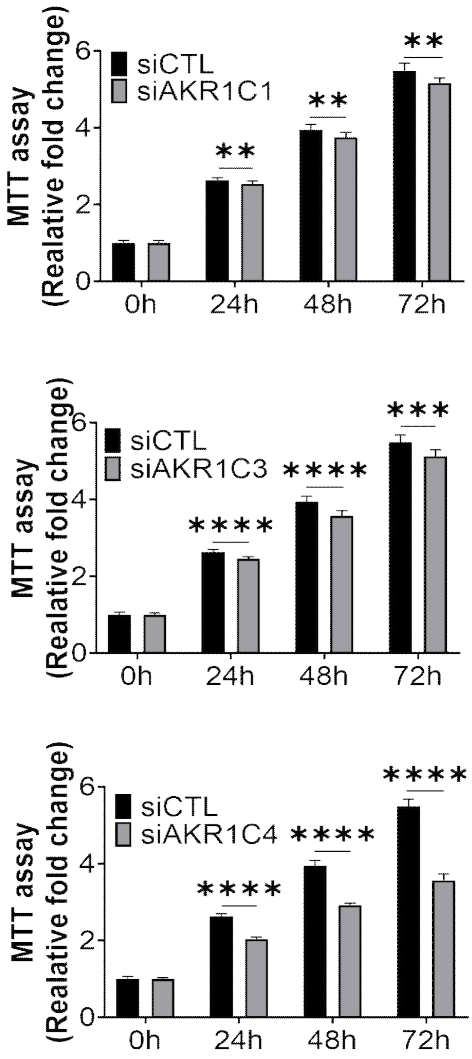

Figure 9. Effect of AKR1C1, AKR1C3, and AKR1C4 silencing on MDA-MB-231 breast cancer cell's proliferation. Error bars denote mean ± SD. $^{*}p \leq 0.05$, $^{**}p \leq 0.01$, $^{***}p \leq 0.001$, $^{****}p \leq 0.0001$. p-values were determined by the Mann-Whitney test.

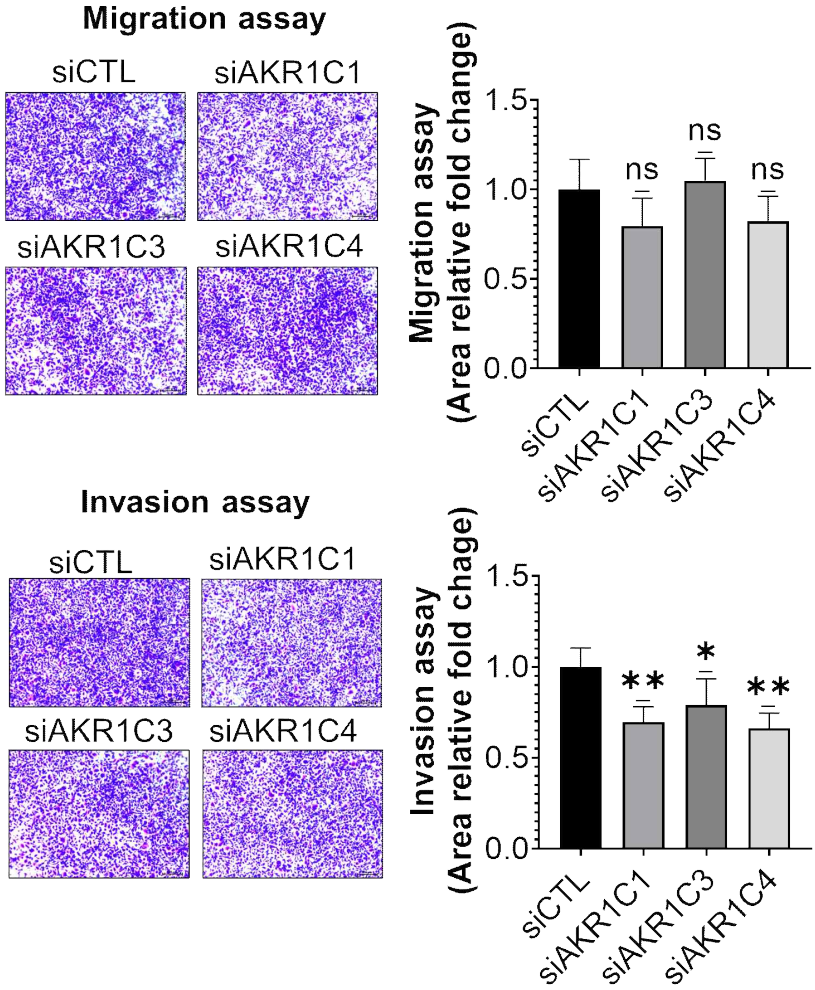

Figure 10. Changes in migratory and invasive abilities after MDA-MB-231 inhibition of AKR1C1, AKR1C3, and AKR1C4. Error bars denote mean ± SD. $^{*}p \leq 0.05$, $^{**}p \leq 0.01$. p-values were determined by the Mann-Whitney test.

AKR1C2 facilitates in vivo tumor growth and lung metastasis for MDA-MD-231 cells.

Next, I tested whether AKR1C2 expression levels affected the growth and metastasis of breast cancer *in vivo*. I transplanted AKR1C2-silenced and control MDA-MB-231 cells into the fat pads of the nude mice (Figure 11A). As shown in Figure 12B-D, AKR1C2 silencing significantly reduced the growth of primary tumors. Furthermore, silencing AKR1C2 resulted in a significantly lower number of spontaneous lung metastases (Figure 12A, 12B). To determine the effect of AKR1C2 on the development of lung metastasis, I additionally performed tail vein injection experiments (Figure 13A) and observed that AKR1C2-silenced breast cancer cells developed a significantly smaller number of lung metastases (Figure 13B, 13C). These data indicate that AKR1C2 regulates primary tumor growth and controls metastasis, which is consistent with the results of the above RNA sequencing data.

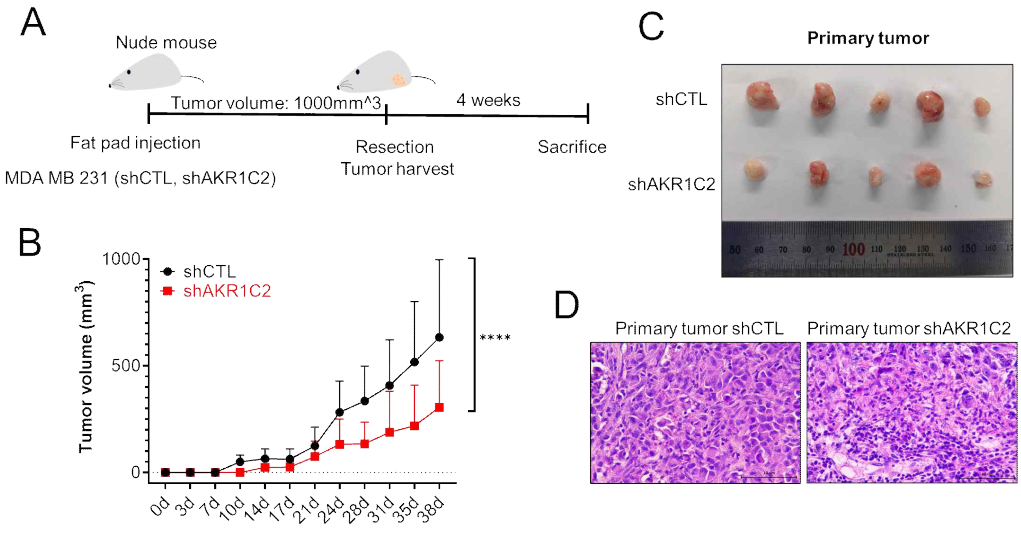

Figure 11. AKR1C2 regulates *in vivo* tumor growth in breast cancer cells. (A) The process of establish xenograft models. **(B)** *In vivo* tumor growth for the control and AKR1C2-silenced MDA-MB-231 cells in nude mice. **(C)** Represent representative images of H&E staining of xenograft tumors. **(D)** Photographs representing xenograft tumors. Error bars denote mean ± SD. $^{****}p \leq 0.0001$. p-values were determined by the Mann-Whitney test.

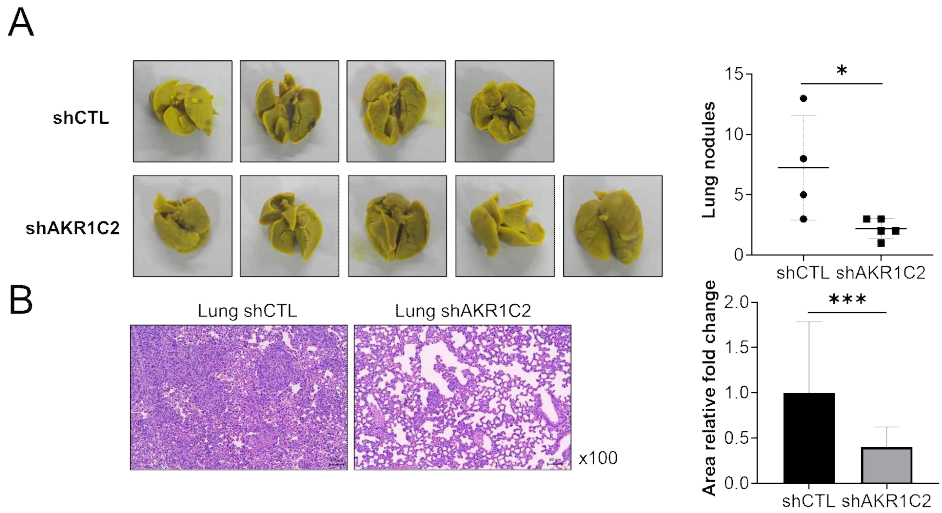

Figure 12. AKR1C2 regulates *in vivo* metastasis of breast cancer cells in xenograft models. (A) The number of metastases were evaluated at one month after the resection of the primary tumors. One of the mice in the control group died during the experiment. **(B)** The area of metastases were evaluated after the resection of the primary tumors. Error bars denote mean ± SD. $^{*}p \leq 0.05$, $^{***}p \leq 0.001$. p-values were determined by the Mann-Whitney test.

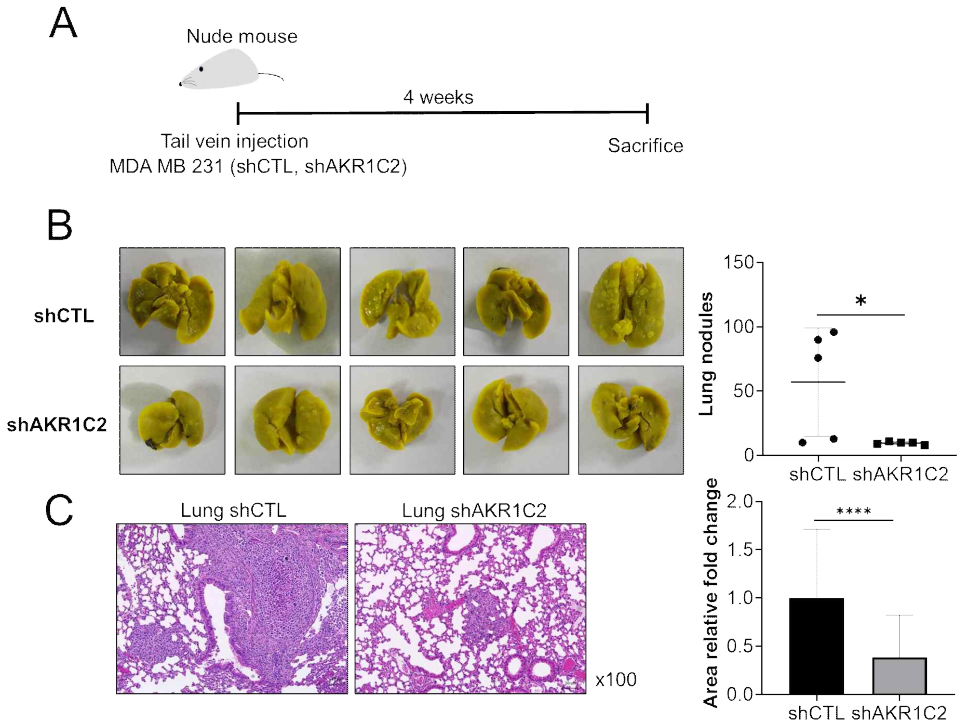

Figure 13. AKR1C2 regulates *in vivo* metastasis of breast cancer cells in lung metastasis xenograft models. (A) The process of establish lung metastasis xenograft models. (B) The number of metastases were evaluated at one month after tail vein injection. (C) The area of metastases were evaluated after the resection of the primary tumors. Error bars denote mean ± SD. $^{*}p \leq 0.05$, $^{****}p \leq 0.0001$. p-values were determined by the Mann-Whitney test.

AKR1C2 is positively associated with LAR subtypes of TNBC.

Steroid hormone biosynthesis regulates the carcinogenesis of TNBC and its molecular classifications [49]. Based on the observation that steroid hormone biosynthesis was the most dysregulated pathway related to the development of distant metastasis and that AKR1C2 plays an important role in cancer cell metastasis *in vivo*, I hypothesized that AKR1C2 can be differentially expressed among the TNBC subtypes. As proposed by Lehmann et al. [20], TNBC can be further classified into six subtypes: two BL (BL1 and BL2), immunomodulatory (IM), mesenchymal (M), mesenchymal stem-like (MSL), and LAR. To test my hypothesis, I obtained gene expression data of 271 TNBC cases from the METABRIC dataset (METABRIC Nature 2012 & Nat Commun 2016) [50] and classified the tumors into different subtypes using the TNBCtype, a web-based subtyping tool for TNBC [51]. The proportions of BL1, BL2, IM, M, MSL, and LAR subtypes were 25.8%, 8.1%, 23.2%, 17.3%, 10.7%, and 14.8%, respectively (Figure 14A). AKR1C2 mRNA levels were significantly different among TNBC subtypes. The LAR subtype showed the highest AKR1C2 levels, whereas the BL1 subtype

showed the lowest levels (Figure 14B).

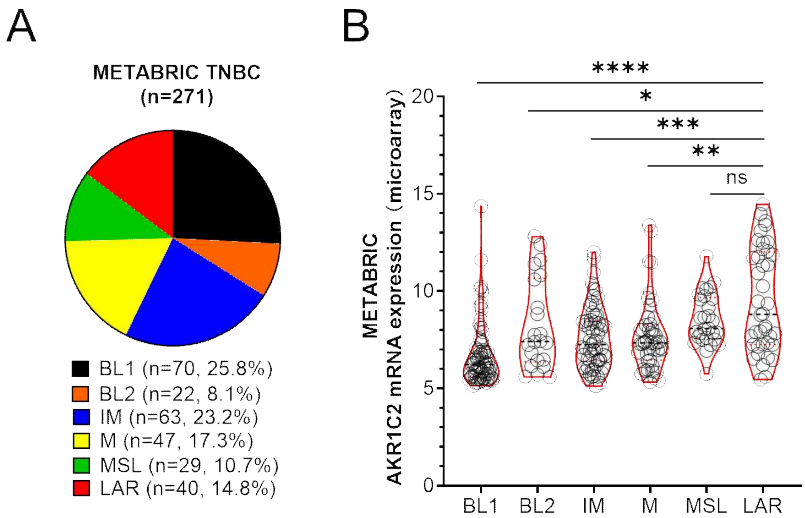

Figure 14. Analysis of TNBC subtypes in the METABRIC dataset. (A) The prevalence of each TNBC subtypes classified by the TNBC type tool using the METABRIC dataset. (B) AKR1C2 mRNA expression levels in TNBC subtypes. Error bars denote mean ± SD. $^{*}p \leq 0.05$, $^{**}p \leq 0.01$, $^{***}p \leq 0.001$ $^{****}p \leq 0.0001$. p-values were determined by the Mann-Whitney test.

Next, I examined the correlation between AKR1C2 and TNBC subtype classifier genes used in the study by Lehman et al. [20]. I observed that genes upregulated in the LAR subtype often showed a positive correlation with AKR1C2, but genes for the BL1 subtype often showed a negative correlation, as representative examples such as PIP for the LAR subtype and CENPF for the BL1 subtype are shown in Figure 15A. When the correlation coefficients for the subtype-defining genes against AKR1C2 were compared, the LAR subtype genes showed significantly higher correlation coefficients when compared to those of the BL1 subtype (Figure 15B).

.

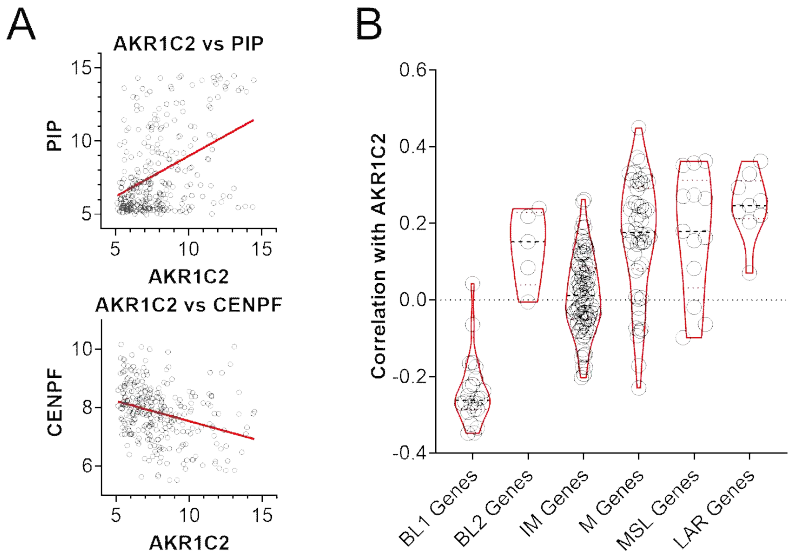

Figure 15. Associations between AKR1C2 and TNBC subtype genes. (A) The scatter plot showing the degree of correlation between AKR1C2 and representative genes from LAR (PIP) or BL1 subtype (CENPF). **(B)** The Spearmen correlation coefficient for the subtype classifier genes and AKR1C2 in TNBC subtypes.

I also measured the mRNA levels of the LAR subtype and BL1 subtype genes in AKR1C2-silenced cells. The expression levels of genes upregulated in the LAR subtype, including AR, were significantly downregulated in AKR1C2-silenced breast cancer cells. In contrast, genes that were upregulated in the BL1 subtype were significantly upregulated in AKR1C2-silenced cells (Figure 16A, 16B). Consistent with previous reports [21, 52], different subtypes of TNBC showed different survival outcomes, with the LAR subtype having the poorest outcomes (Figure 17, Table 6). These data indicated that AKR1C2 may play a critical role in determining the subtype characteristics of TNBC cells.

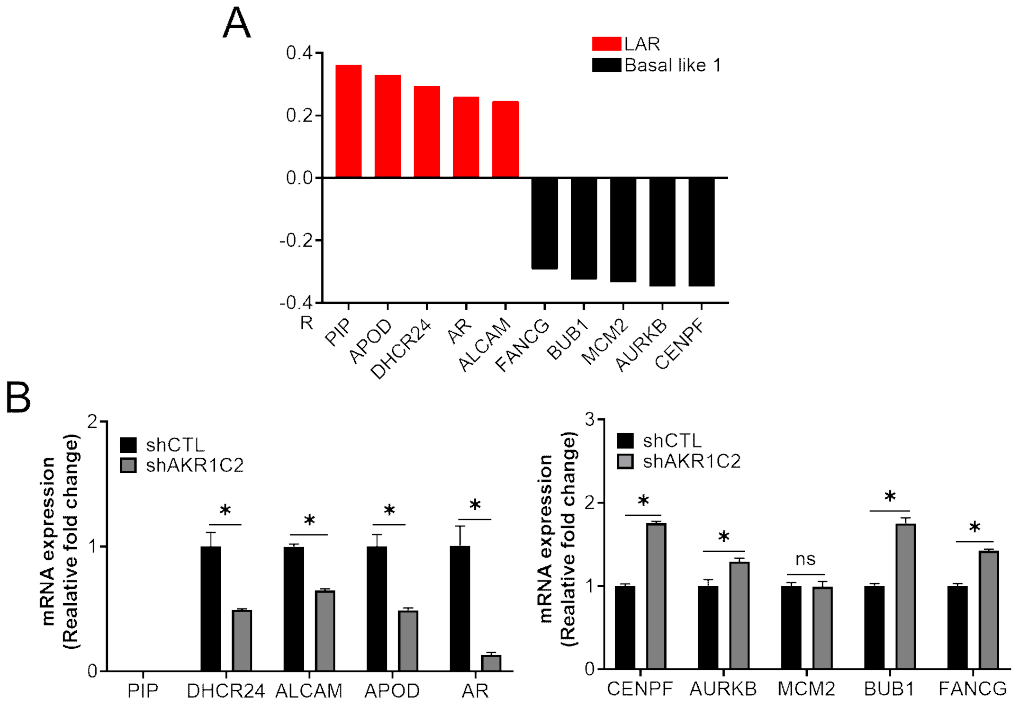

Figure 16. Expression of LAR and Basal like1 related genes in AKR1C2-silenced MDA-MB-231. (A) The top five LAR subtype-related genes and BL1 subtype-related genes with the highest correlation coefficient R after AKR1C2 correlation analysis. **(B)** mRNA expression of these genes in AKR1C2-silenced MDA-MB-231. Error bars denote mean ± SD. ns = not significant, $^{*}p \leq 0.05$. p-values were determined by the Mann-Whitney test.

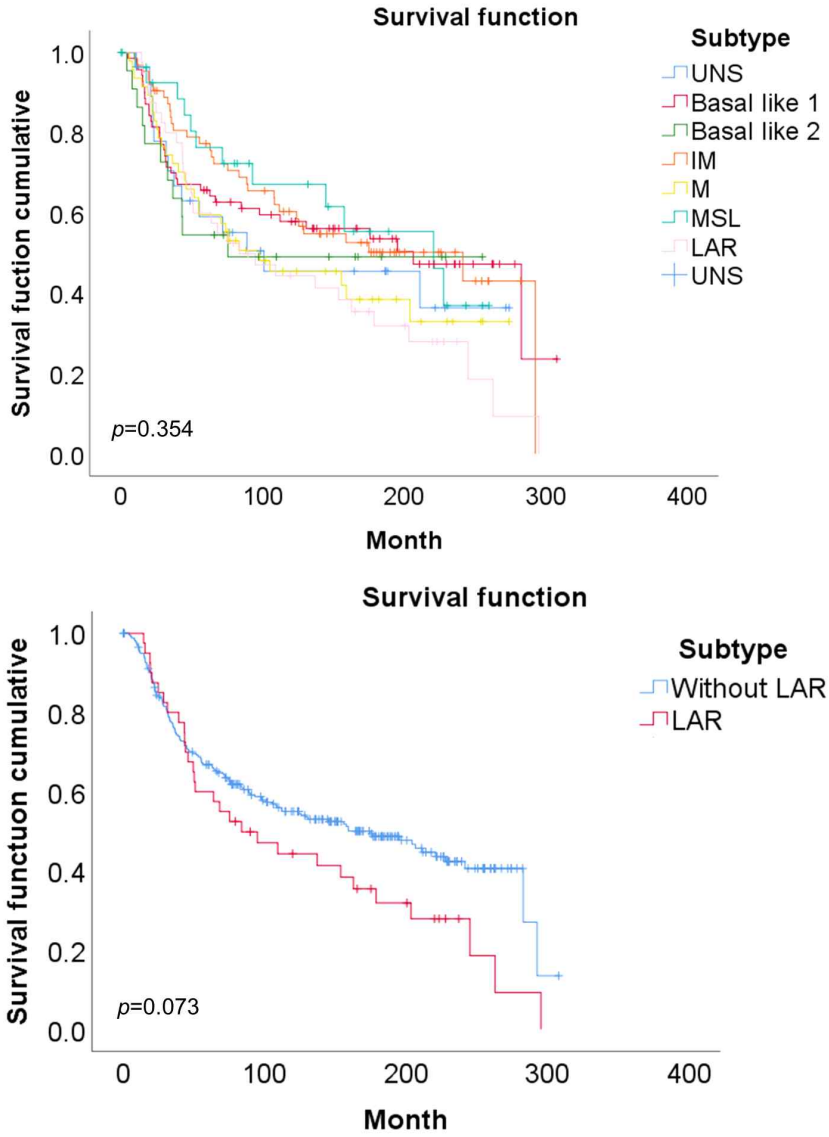

Figure 17. Survival function of TNBC subtypes. *p*-values were determined by Spearman correlation,Mann-Whitney, andlog-rank test.

Table 6. The median and mean survival times of TNBC subtypes in the METABRIC dataset

Median

UNS	BL1	BL2	IM	M	MSL	LAR		Subtype median (month)
	195.4 (90.5–300.2)	101.1 (0–245)	175.1 (82.5–267.7)	98.1 (17.2–179)	211.2 (82.4–340)	94.9 (52.3–137.6)	UNS	101.1
		195.4 (135.1–255.6)	206.6 (103.3–309.9)	159.2 (77.3–241.2)	206.6 (138.4–274.7)	153.8 (80.5–227.1)	BL1	206.6
			175.1 (70–280.2)	98.1 (15.9–180.3)	220.9 (130.4–311.4)	83.7 (11.3–156.1)	BL2	75.5
				155.7 (85.7–225.8)	220.9 (138.3–303.5)	137.1 (76.5–197.7)	IM	241.6
					155.7 (88.8–222.7)	94.9 (58.2–131.6)	M	98.1
						144.7 (74.5–214.8)	MSL	220
							LAR	83.7

Mean

UNS	BL1	BL2	IM	M	MSL	LAR		Subtype mean (month)
	168 (141.2–194.7)	146 (112.2–179.8)	170 (144.6–195.5)	139.5 (113.5–165.6)	159.5 (129.1–189.9)	137 (109.4–164.6)	UNS	143.2
		170.1 (142.1–198)	176.2 (154.3–198)	161.9 (137.7–186.2)	176.6 (150.3–202.9)	156.1 (133–179.2)	BL1	174.2
			172.4 (145.7–199)	140.2 (112.5–167.9)	157.6 (126.9–188.3)	134.2 (105.4–163)	BL2	140.3
				163.1 (140.2–186.1)	179.5 (154.7–204.3)	157.5 (134.9–180)	IM	179.3
					150.3 (124.6–175.9)	134.9 (110.9–159)	M	136.8
						147.3 (120.5–174)	MSL	171.6
							LAR	129.2

AR, a gene regulated by AKR1C2, controls the proliferation and migration of TNBC cells.

AR is a major driver of the molecular features of the LAR subtype in TNBC [48]. I observed decreased AR expression in AKR1C2-silenced breast cancer cells (Figure 18A). However, AKR1C2 levels were not changed in AR-silenced MDA-MB-231 cells, suggesting an upstream role of AKR1C2 in regulating AR levels (Figure 18B). Next, I performed in vitro assays to determine whether AKR1C2-mediated regulation of AR in breast cancer cells plays a role in the phenotypes observed in AKR1C2-silenced cells. When cells were treated with siAR, MDA-MB-231 cells showed a significant reduction in cell proliferation (Figure 19). Additionally, siAR-treated cells showed decreased transwell migration and Matrigel invasion (Figure 20A, 20B). These data indicate that, at least in part, the phenotypes associated with AKR1C2 silencing may be the result of AKR1C2-mediated AR regulation in breast cancer cells.

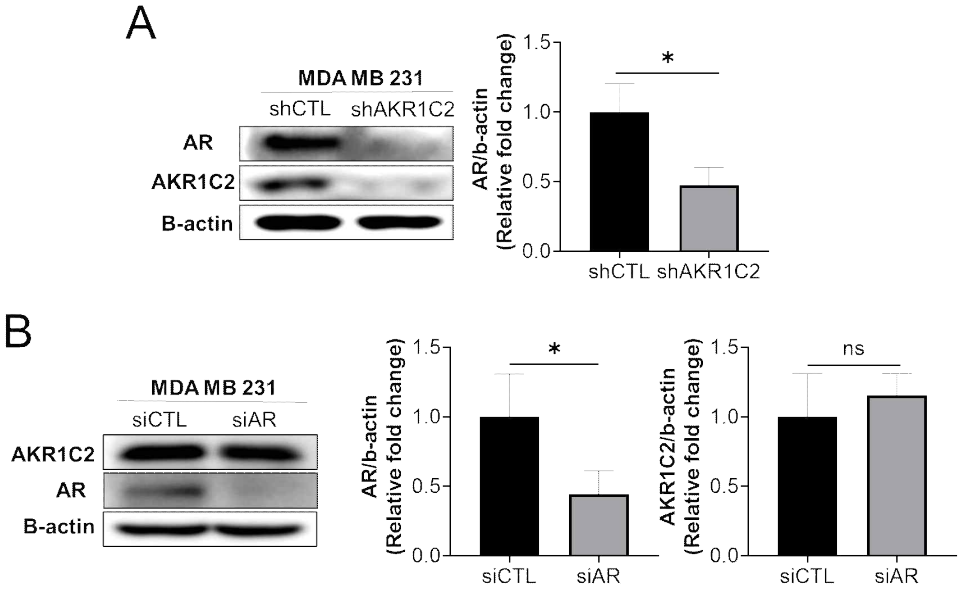

Figure 18. Effects of silencing AKR1C2 on AR expression in MDA-MB-231. (A) AR protein expression levels in AKR1C2-silenced MDA-MB-231 cells. (B) AKR1C2 protein expression levels in AR-silenced MDA-MB-231 cells. Error bars denote mean ± SD. ns = not significant, $^{*}p \leq 0.05$. p-values were determined by the Mann-Whitney test.

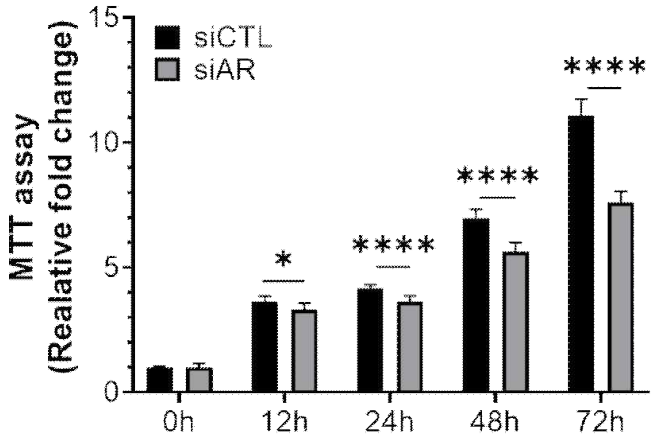

Figure 19. Effect of AR silencing on MDA-MB-231 breast cancer cell' s proliferation. Error bars denote mean ± SD. $^{*}p \leq 0.05$, $^{****}p \leq 0.0001$. p-values were determined by the Mann-Whitney test.

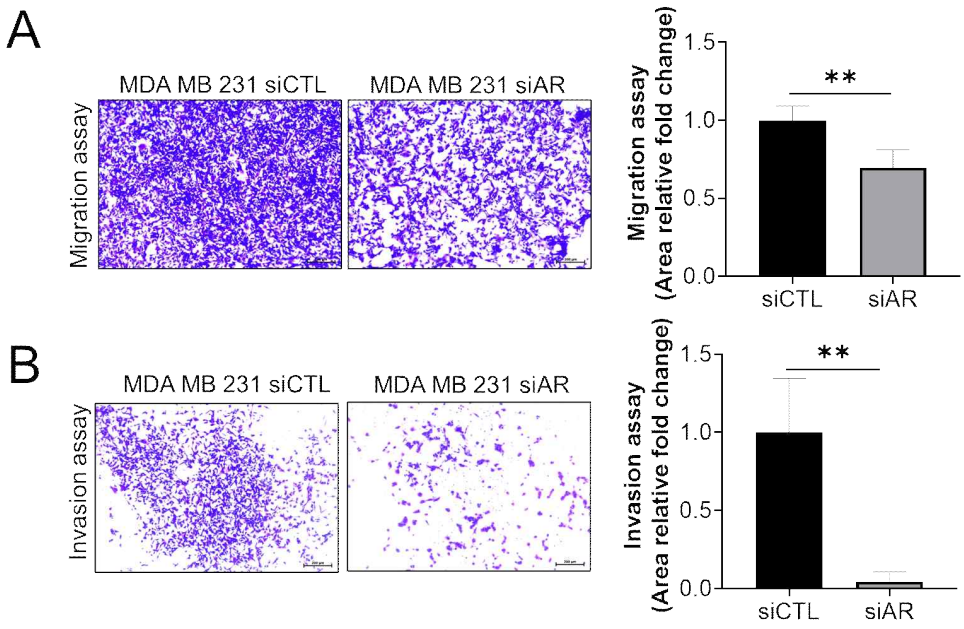

Figure 20. Effect of AR silencing on MDA-MB-231 breast cancer cell's migration and invasion. (A) Changes in migratory after MDA-MB-231 inhibition of AR. (B) Changes in invasive abilities after MDA-MB-231 inhibition of AR. Error bars denote mean ± SD. $^{**}p \leq 0.01$. p-values were determined by the Mann-Whitney test.

Studies [53, 54] have shown that AR can be regulated by activated STAT3. Based on the RNA sequencing data comparing the gene expression profiles of AKR1C2-silenced MDA-MB-231 cells to those of control MDA-MB-231 cells (Figure 21A), I observed that the genes involved in the JAK-STAT signaling pathway were significantly dysregulated in AKR1C2-silenced cells (Figure 21B). Additionally, AKR1C2-silenced cells showed significantly reduced STAT3 phosphorylation (Figure 22). Dong et al. [55] suggested a reciprocal interaction between AR and IL-6 which is regulated by STAT3 signaling. Consistently, I observed that AKR1C2-silencing resulted in the downregulation of IL-6 protein (Figure 23A) and mRNA (Figure 23B) levels in breast cancer cells. ELISA results indicated that the amount of secreted IL-6 was also significantly reduced in AKR1C2-silenced cells (Figure 22C).

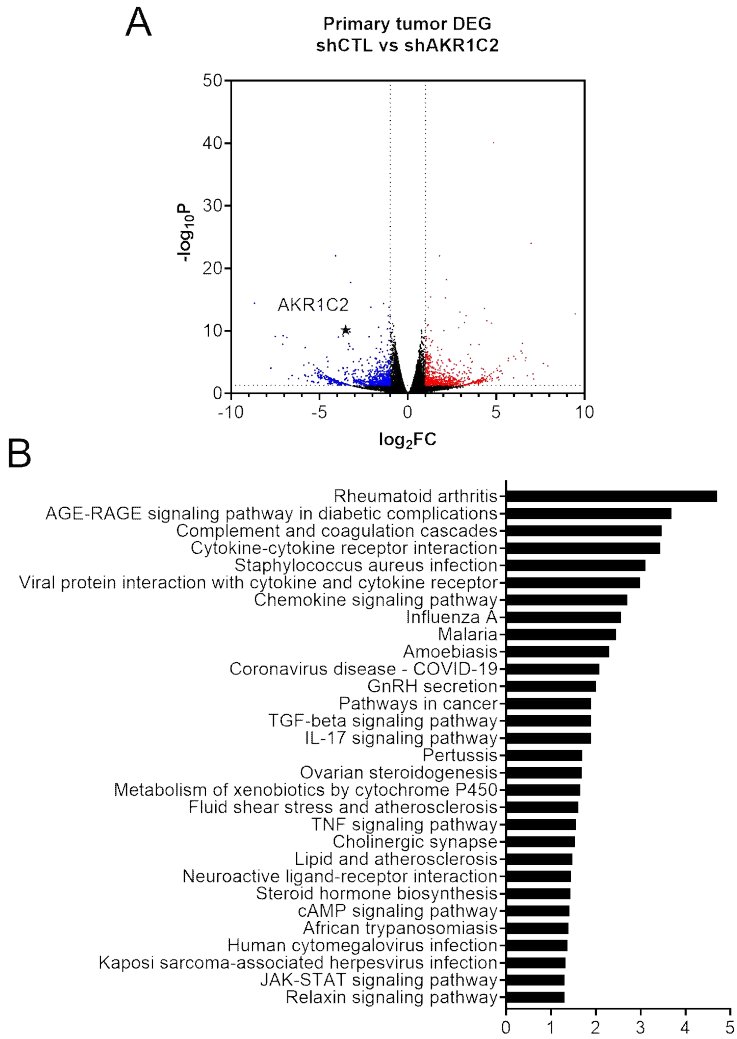

Figure 21. Results of RNA sequencing of primary tumors in xenograft models. (A) The volcano plot illustrates the down-regulation of AKR1C2. (B) KEGG pathway analysis of downregulated genes in xenograft tumor tissues.

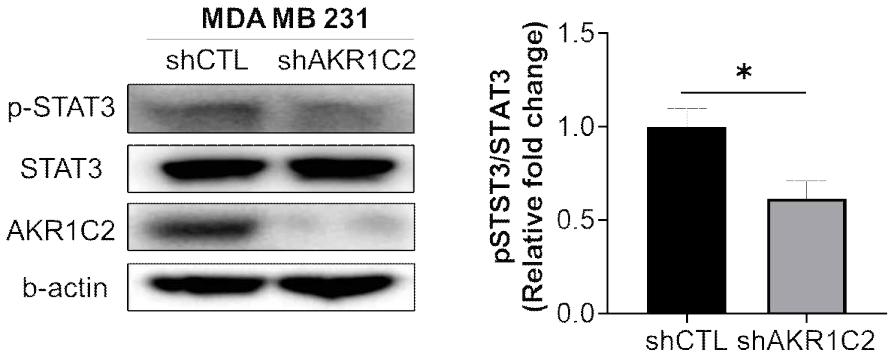

Figure 22. pSTAT3 and STAT3 protein expression levelsin AKR1C2-silenced MDA-MB-231 cells. Error bars denote mean ± SD. $^{*}p \leq 0.05$. p-values were determined by the Mann-Whitney test.

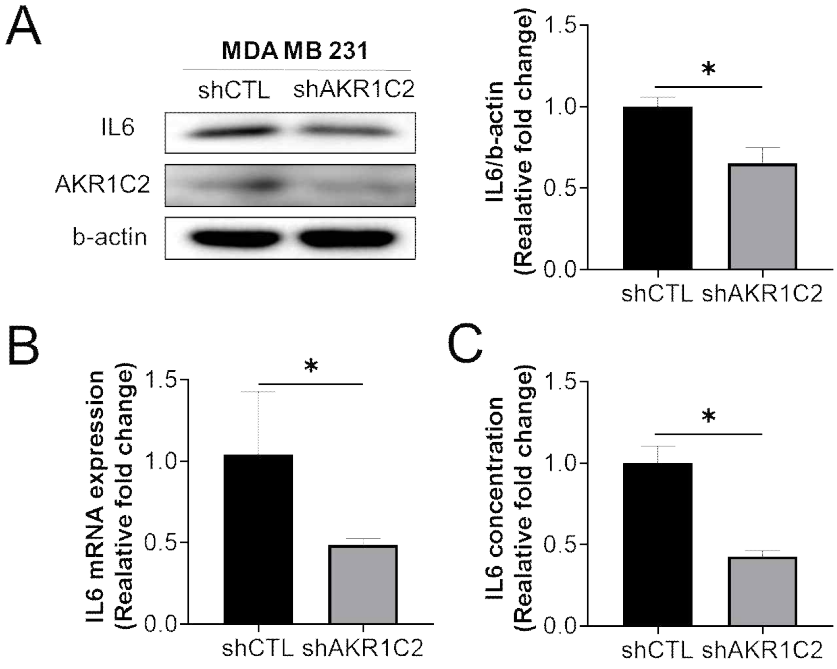

Figure 23. IL6 expression and secretion in AKR1C2-silenced MDA-MB-231 cells. (A) IL-6 protein expression levels in AKR1C2-silenced MDA MB 231 cells. **(B)** IL-6 mRNA expression levelsin AKR1C2-silenced MDA-MB-231 cells. **(C)** IL-6 concentration in AKR1C2-silenced MDA-MB-231-conditioned medium. Error bars denote mean ± SD. $^{*}p \leq 0.05$. p-values were determined by the Mann-Whitney test.

IV. Discussion

In the present study, I attempted to identify the genes associated with breast cancer metastasis using primary tumor tissues and their corresponding PDX tumor tissues. As one can efficiently separate gene expression data originating from epithelial tumor cells and surrounding microenvironment cells [45], integrated analysis of primary tumors and PDX tumors may provide more accurate information on the molecular profiles of epithelial cancer cells. This approach has revealed the importance of JAK2 signaling in regulating paclitaxel resistance in TNBC [18], and Mastri et al. showed that patient-derived models may allow the analysis of epithelial cancer cell pathways independent of the tumor microenvironment [46]. Additionally, the molecular characteristics of the tumor cells are relatively well preserved in the PDX tumor cells [9, 15, 18, 45, 46, 56], and for some instances, PDX tumors may represent the nature of metastatic clones better than primary tumor tissues [57].

Using this approach, including primary and PDX tumor tissues of 31 patients with breast cancer, I identified AKR1C2 as a potential regulator of distant metastasis in breast cancer. AKR1C2 promoted cancer cell proliferation, migration, and

invasion *in vitro*, and AKR1C2 facilitated tumor growth and metastasis *in vivo*. In this study, I believe that the candidate gene AKR1C2 may promote breast cancer metastasis. According to previous research, AKR1C2 can catalyze the conversion of dihydrotestosterone (DHT) to 5α-androstane-3α,17β-diol (3α-diol) [58]. And affects a variety of tumor types (Table 7). AKR1C2 has been proposed in esophageal cancer, liver cancer and other studies to not only affect the PI3K/Akt and STAT3 signaling pathways [59, 60], but may also affect EMT-related proteins [61, 62]. However, the role of AKR1C2 in breast cancer, especially triple-negative breast cancer, is rarely studied. In this study, I confirmed that AKR1C2 plays an important role in the progression of TNBC through *in vivo* and *in vitro* experiments.

Table 7. The role of AKR1C2 in tumor

Tumor type	Reference	Affected pathway	Promote tumor progression	Suppress tumor progression
Esophageal squamous cell carcinoma	Zhang, et al. 2020 [60]	PI3K/Akt signaling pathway	O	
Liver Cancer	Li, et al. 2016 [62]	EMT(E-cadherin)	O	
Prostate cancer	Rizner, et al. 2003 [63]	DHT metabolism		O
Lung cancer	Zhu, et al. 2018 [59]	STAT3 pathway	O	
Endometrial cancer	Sinreih, et al. 2015 [64]	Progesterone metabolism	O	

AKR1C1-4, four members of the aldo-keto reductase family 1 member C (AKR1C) family, is expressed in different degrees in various tissues in the human body. Its main function is to participate in the production and metabolism of steroids and sex hormones [58]. Studies have shown that AKR1C1-4 is associated with the progression of various tumors, such as lung, liver, and nasopharyngeal cancer [59, 65, 66]. These genes can affect tumor cells by activating and regulating the activity of PI3K/AKT, JAK-STAT, and NF-kb signaling pathway [62, 65-68]. To further understand the role of these family members

in TNBC, I inhibited AKR1C1, AKR1C3, and AKR1C4 in MDA-MB-231 and performed activity, metastasis and invasion assay. In this study, other members of the AKR1C family had corresponding effects on breast cancer progression, but less significantly than AKR1C2. My data indicate that AKR1C2, a steroid hormone biosynthesis gene that catalyzes NADH and NADPH-dependent conversion of dihydrotestosterone to 3α-diol, may play a more important role in the development of distant metastasis of TNBC than other AKR1C family members.

However, the role of AKR1C2 in various solid tumor types remains controversial. It has been reported that in malignant tumors, such as prostate cancer and esophageal cancer, AKR1C2 can promote tumor growth and metastasis by regulating epithelial mesenchymal transition or affecting the phosphoinositide 3-kinase (PI3K)/Akt signaling pathway [60, 62, 69]. Although I observed similar pro-tumorigenic effects of AKR1C2 in TNBC cells in the present study, AKR1C2 had no effect on PI3K/Akt signaling in TNBC cells. In this study, AKR1C2 was shown to regulate AR expression. Studies have shown that AKR1C2 can directly interact with STAT3 and phosphorylate STAT3 [59]. pSTAT3 can modulate AR activation in the absence of hormones [53, 54, 70]. I obtained downregulated genes in the experimental group by RNA-sequencing primary tumors from xenograft

models. And through KEGG pathway analysis and Western blots, it was found that AKR1C2 affect the JAK-STAT pathway and phosphorylate STAT3.

In the present study, AKR1C2 affected the JAK-STAT pathway and pSTAT3. This may be the mechanism that affects TNBC metastasis. On the other hand, some studies have suggested that AKR1C2 may exert inhibitory effects on tumors, as AKR1C2 expression is associated with improved prognosis in thyroid cancer [71] and AKR1C2 overexpression results in slower tumor growth in prostate cancer [63, 72]. Further research on the role of AKR1C2 in human solid tumors is required to clarify its importance in different tumor types.

Additionally, my data suggested that AKR1C2 may influence the subtype determination of TNBC cells. Although efforts have been made to clarify the origins of the different intrinsic subtypes of breast cancer [73, 74], the molecular mechanisms underlying the classification of the TNBC subtype are largely unknown. Since Lehman et al. [20]proposed that TNBC can be further classified into different subtypes, studies have repeatedly shown the presence of heterogeneity and its clinical implications [52, 75]. In the present study, AKR1C2 was highly upregulated in the LAR subtype, whereas it was significantly downregulated in the BL1 subtype. Furthermore, AKR1C2 silencing resulted in

the downregulation of genes expressed in the LAR subtype, including AR. These observations indicate that AKR1C2 expression levels may determine the subtypes of TNBC cells, as PDGF signaling is suggested to regulate the conversion of basal breast cancer to luminal cancer [76]. And through the analysis of METABRIC TNBC dataset, it was found that the prognosis of patients with LAR subtype is the poorest among all subtypes. These results indicate that AKR1C2 may affect breast cancer progression by altering TNBC subtypes. Of course, the potential association between AKR1C2 and LAR subtypes and their therapeutic implications should be tested in future studies.

My study has several limitations. First, although my data suggest that AKR1C2 regulates AR expression, the mechanism by which it affects AR has not yet been elucidated. Second, I could not address the functional importance of AKR1C2 in non-basal subtypes because I focused my assays on TNBC cell lines. Finally, I was unable to determine the prognostic importance of AKR1C2 in an independent cohort of patients with breast cancer.

V. Conclusion

In conclusion, my data indicated that AKR1C2 is an important regulator of cancer growth and metastasis in TNBC cells. AKR1C2 regulates the expression of AR in breast cancer cells and is associated with the LAR subtype of TNBC. Future research on the potential therapeutic use of targeting AKR1C2 in patients with TNBC is warranted.

VI. References

1. H. Sung, J. Ferlay, R. L. Siegel, M. Laversanne, I. Soerjomataram, A. Jemal, et al. Global cancer statistics 2020: GLOBOCAN estimates of incidence and mortality worldwide for 36 cancers in 185 countries. CA Cancer J Clin 2021;71:209-49.
2. Jung KW, Won YJ, Hong S, Kong HJ, Im JS, Seo HG. Prediction of cancer incidence and mortality in korea, 2021. Cancer Res Treat 2021;53:316-22.
3. Kang SY, Lee SB, Kim YS, Kim Z, Kim HY, Kim HJ, et al. Breast cancer statistics in Korea, 2018. J Breast Cancer 2021;24:123-37.
4. Lee SB, Kim HK, Choi Y, Ju YW, Lee HB, Han W, et al. Dynamic and subtype-specific interactions between tumour burden and prognosis in breast cancer. Sci Rep 2020;10:15445.
5. Kumar P, Aggarwal R. An overview of triple-negative breast cancer. Arch Gynecol Obstet 2016;293:247-69.
6. Foulkes WD, Smith IE, Reis-Filho JS. Triple-negative breast cancer. N Engl J Med 2010;363:1938-48.
7. Dent R, Trudeau M, Pritchard KI, Hanna WM, Kahn HK,

Sawka CA, et al. Triple-negative breast cancer: clinical features and patterns of recurrence. Clin Cancer Res 2007;13:4429-34.

8. Shi J, Li Y, Jia R, Fan X. The fidelity of cancer cells in PDX models: Characteristics, mechanism and clinical significance. Int J Cancer 2020;146:2078-88.

9. Eirew P, Stief A, Khattra J, Ha G, Yap D, Farahani H, et al. Dynamics of genomic clones in breast cancer patient xenografts at single-cell resolution. Nature 2015;518:422-6.

10. Okada S, Vaeteewoottacharn K, Kariya R. Application of highly immunocompromised mice for the establishment of patient-derived xenograft (PDX) models. Cells 2019;8:889.

11. Aparicio S, Hidalgo M, Kung AL. Examining the utility of patient-derived xenograft mouse models. Nat Rev Cancer 2015;15:311-6.

12. Byrne AT, Alferez DG, Amant F, Annibali D, Arribas J, Biankin AV, et al. Interrogating open issues in cancer precision medicine with patient-derived xenografts. Nat Rev Cancer 2017;17:254-68.

13. Blomme A, Van Simaeys G, Doumont G, Costanza B, Bellier J, Otaka Y, et al. Murine stroma adopts a

human-like metabolic phenotype in the PDX model of colorectal cancer and liver metastases. Oncogene 2018; 37:1237-50.

14. Yoshida GJ. Applications of patient-derived tumor xenograft models and tumor organoids. J Hematol Oncol 2020;13:4.

15. Moon HG, Oh K, Lee J, Lee M, Kim JY, Yoo TK, et al. Prognostic and functional importance of the engraftment-associated genes in the patient-derived xenograft models of triple-negative breast cancers. Breast Cancer Res Treat 2015;154:13-22.

16. Jung J, Seol HS, Chang S. The Generation and application of patient-derived xenograft model for cancer research. Cancer Res Treat 2018;50:1-10.

17. Kerbel RS. Human tumor xenografts as predictive preclinical models for anticancer drug activity in humans-better than commonly perceived-but they can be improved. Cancer Biology & Therapy 2003;2:S134-9.

18. Han J, Yun J, Quan M, Kang W, Jung JG, Heo W, et al. JAK2 regulates paclitaxel resistance in triple negative breast cancers. J Mol Med (Berl) 2021;99;1783-95.

19. DeRose YS, Wang G, Lin YC, Bernard PS, Buys SS, Ebbert MT, et al. Tumor grafts derived from women with

breast cancer authentically reflect tumor pathology, growth, metastasis and disease outcomes. Nat Med 2011;17:1514-20.

20. Lehmann BD, Bauer JA, Chen X, Sanders ME, Chakravarthy AB, Shyr Y, et al. Identification of human triple-negative breast cancer subtypes and preclinical models for selection of targeted therapies. J Clin Invest 2011;121:2750-67.

21. Lehmann BD, Jovanović B, Chen X, Estrada MV, Johnson KN, Shyr Y, et al. Refinement of Triple-Negative Breast Cancer Molecular Subtypes: Implications for Neoadjuvant Chemotherapy Selection. PLoS One 2016;11:e0157368.

22. Sutton LM, Cao D, Sarode V, Molberg KH, Torgbe K, Haley B, et al. Decreased androgen receptor expression is associated with distant metastases in patients with androgen receptor-expressing triple-negative breast carcinoma. Am J Clin Pathol 2012;138:511-6.

23. Thike AA, Yong-Zheng Chong L, Cheok PY, Li HH, Wai-Cheong Yip G, Huat Bay B, Tse GM, et al. Loss of androgen receptor expression predicts early recurrence in triple-negative and basal-like breast cancer. Mod Pathol 2014;27:352-60.

24. Culig Z, Santer FR. Androgen receptor signaling in

prostate cancer. Cancer and Metastasis Rev 2014;33:413-27.

25. Yeh S, Hu YC, Wang PH, Xie C, Xu Q, Tsai MY, et al. Abnormal mammary gland development and growth retardation in female mice and MCF7 breast cancer cells lacking androgen receptor. J Exp Med 2003;198:1899-908.

26. Feng J, Li L, Zhang N, Liu J, Zhang L, Gao H, et al. Androgen and AR contribute to breast cancer development and metastasis: an insight of mechanisms. Oncogene 2017;36:2775-90.

27. Anestis A, Zoi I, Papavassiliou AG, Karamouzis MV. Androgen receptor in breast cancer-clinical and preclinical research insights. Molecules 2020;25:358.

28. Pistelli M, Caramanti M, Biscotti T, Santinelli A, Pagliacci A, De Lisa M, et al. Androgen receptor expression in early triple-negative breast cancer: clinical significance and prognostic associations. Cancers (Basel) 2014;6:1351-62.

29. McGhan LJ, McCullough AE, Protheroe CA, Dueck AC, Lee JJ, Nunez-Nateras R, et al. Androgen receptor-positive triple negative breast cancer: a unique breast cancer subtype. Ann Surg Oncol 2014;21:361-7.

30. Gasparini P, Fassan M, Cascione L, Guler G, Balci S, Irkkan C, Androgen receptor status is a prognostic marker in non-basal triple negative breast cancers and determines novel therapeutic options. PLoS One 2014;9:e88525.

31. Burstein MD, Tsimelzon A, Poage GM, Covington KR, Contreras A, Fuqua SA, et al. Comprehensive genomic analysis identifies novel subtypes and targets of triple-negative breast cancer. Clin Cancer Res 2015;21:1688-98.

32. Choi JE, Kang SH, Lee SJ, Bae YK. Androgen receptor expression predicts decreased survival in early stage triple-negative breast cancer. Ann Surg Oncol 2015; 22:82-9.

33. Ricciardi GR, Adamo B, Ieni A, Licata L, Cardia R, Ferraro G, et al. Androgen receptor (AR), E-cadherin, and Ki-67 as emerging targets and novel prognostic markers in triple-negative breast cancer (TNBC) Patients. PLoS One 2015;10:e0128368.

34. Asano Y, Kashiwagi S, Onoda N, Kurata K, Morisaki T, Noda S, et al. Clinical verification of sensitivity to preoperative chemotherapy in cases of androgen receptor-expressing positive breast cancer. Br J Cancer

2016;114:14-20.

35. Asano Y, Kashiwagi S, Goto W, Tanaka S, Morisaki T, Takashima T, et al. Expression and clinical significance of androgen receptor in triple-negative breast cancer. Cancers (Basel) 2017;9:4.

36. Hu XQ, Chen WL, Ma HG, Jiang K. Androgen receptor expression identifies patient with favorable outcome in operable triple negative breast cancer. Oncotarget 2017; 8:56364-74.

37. Bareche Y, Venet D, Ignatiadis M, Aftimos P, Piccart M, Rothe F, et al. Unravelling triple-negative breast cancer molecular heterogeneity using an integrative multiomic analysis. Ann Oncol 2018;29:895-902.

38. Astvatsaturyan K, Yue Y, Walts AE, Bose S. Androgen receptor positive triple negative breast cancer: Clinicopathologic, prognostic, and predictive features. PLoS One 2018;13:e0197827.

39. Sunar V, T Dogan H, Sarici F, Ates O, Akin S, Baspinar B, et al. Association between androgen receptor status and prognosis in triple negative breast cancer. J BUON 2018;23:1325-30.

40. Dieci MV, Tsvetkova V, Griguolo G, Miglietta F, Mantiero M, Tasca G, et al. Androgen receptor expression and

association with distant disease-free survival in triple negative breast cancer: Analysis of 263 patients treated with standard therapy for stage I-III disease. Front Oncol 2019;9:452.

41. Mangia A, Saponaro C, Vagheggini A, Opinto G, Centonze M, Vicenti C, et al. Should tumor infiltrating lymphocytes, androgen receptor, and FOXA1 expression predict the clinical outcome in triple negative breast cancer patients? Cancers (Basel), 2019;11:1393.

42. Bhattarai S, Klimov S, Mittal K, Krishnamurti U, Li XB, Oprea-Ilies G, et al. Prognostic Role of Androgen Receptor in Triple Negative Breast Cancer: A Multi-Institutional Study. Cancers (Basel) 2019;11:995.

43. Govindan S, Siraganahalli Eswaraiah M, Basavaraj C, Adinarayan M, Sankaran S, Bakre M. Androgen Receptor mRNA levels determine the prognosis in triple-negative breast cancer patients. BMC Cancer 2020;20:745.

44. Lyalkin SA, Verevkina NO, Alekseyenko OO, Syvak LA. Prognostic role of androgen receptor expression in patients with metastatic triple negative breast cancer. Exp Oncol 2020;42:140-143.

45. Cho SY, Chae J, Na D, Kang W, Lee A, Min S, et al. Unstable Genome and Transcriptome Dynamics during

Tumor Metastasis Contribute to Therapeutic Heterogeneity in Colorectal Cancers. Clin Cancer Res 2019;25:2821-34.

46. Mastri M, Ramakrishnan S, Shah SD, Karasik E, Gillard BM, Moser MT, et al. Patient derived models of bladder cancer enrich the signal of the tumor cell transcriptome facilitating the analysis of the tumor cell compartment. Am J Clin Exp Urol 2021;9:416-34.

47. Tchernof A, Mansour MF, Pelletier M, Boulet MM, Nadeau M, Luu-The V. Updated survey of the steroid-converting enzymes in human adipose tissues. J Steroid Biochem Mol Biol 2015;147:56-69.

48. Penning TM, Byrns MC. Byrns, Steroid hormone transforming aldo-keto reductases and cancer. Ann N Y Acad Sci 2009;1155:33-42.

49. Christenson JL, Trepel JB, Ali HY, Lee S, Eisner JR, Baskin-Bey ES, et al. Harnessing a Different Dependency: How to Identify and Target Androgen Receptor-Positive Versus Quadruple-Negative Breast Cancer. Horm Cancer 2018;9:82-94.

50. Curtis C, Shah SP, Chin SF, Turashvili G, Rueda OM, Dunning MJ, et al. The genomic and transcriptomic architecture of 2,000 breast tumours reveals novel

subgroups. Nature 2012;486:346-52.

51. Chen X, Li J, Gray WH, Lehmann BD, Bauer JA, Shyr Y, et al. TNBCtype: A subtyping tool for triple-negative breast cancer. Cancer Inform 2012;11:147-56.

52. Lehmann BD, Colaprico A, Silva TC, Chen J, An H, Ban Y, et al. Multi-omics analysis identifies therapeutic vulnerabilities in triple-negative breast cancer subtypes. Nat Commun 2021;12:6276.

53. Hobisch A, Eder IE, Putz T, Horninger W, Bartsch G, Klocker H, et al. Interleukin-6 regulates prostate-specific protein expression in prostate carcinoma cells by activation of the androgen receptor. Cancer Res 1998;58:4640-5.

54. Lee SO, Lou W, Hou M, de Miguel F, Gerber L, Gao AC. Interleukin-6 promotes androgen-independent growth in LNCaP human prostate cancer cells. Clin Cancer Res, 2003;9:370-6.

55. Dong H, Xu J, Li W, Gan J, Lin W, Ke J, et al. Reciprocal androgen receptor/interleukin-6 crosstalk drives oesophageal carcinoma progression and contributes to patient prognosis. J Pathol 2017;241:448-462.

56. Kopetz S, Lemos R, Powis G. The promise of patient-derived xenografts: the best laid plans of mice

and men. Clin Cancer Res 2012;18:5160-2.

57. Ding L, Ellis MJ, Li S, Larson DE, Chen K, Wallis JW, et al. Genome remodelling in a basal-like breast cancer metastasis and xenograft. Nature 2010;464:999-1005.

58. Penning TM, Burczynski ME, Jez JM, Hung CF, Lin HK, Ma H, et al. Human 3alpha-hydroxysteroid dehydrogenase isoforms (AKR1C1-AKR1C4) of the aldo-keto reductase superfamily: functional plasticity and tissue distribution reveals roles in the inactivation and formation of male and female sex hormones. Biochem J 2000;351:67-77.

59. Zhu H, Chang LL, Yan FJ, Hu Y, Zeng CM, Zhou TY, et al. AKR1C1 activates STAT3 to promote the metastasis of non-small cell lung cancer. Theranostics 2018;8:676-692.

60. Zhang ZF, Huang TJ, Zhang XK, Xie YJ, Lin ST, Luo FF, et al. AKR1C2 acts as a targetable oncogene in esophageal squamous cell carcinoma via activating PI3K/AKT signaling pathway. J Cell Mol Med 2020;24:9999-10012.

61. Li C, Wu X, Zhang W, Li J, Liu H, Hao M, et al. AEG-1 promotes metastasis through downstream AKR1C2 and NF1 in liver cancer. Oncology Research 2014;22:203-11.

62. Li C, Wu X, Zhang W, Li J, Liu H, Hao M, et al. High-content functional screening of AEG-1 and AKR1C2 for the promotion of metastasis in liver cancer. J Biomol Screen 2016;21:101-7.

63. Rizner TL, Lin HK, Penning TM. Role of human type 3 3alpha-hydroxysteroid dehydrogenase (AKR1C2) in androgen metabolism of prostate cancer cells. Chem Biol Interact 2003;143-144:401-9.

64. Sinreih M, Anko M, Zukunft S, Adamski J, Rižner TL. Important roles of the AKR1C2 and SRD5A1 enzymes in progesterone metabolism in endometrial cancer model cell lines. Chem Biol Interact 2015;234:297-308.

65. Zhou Q, Tian W, Jiang Z, Huang T, Ge C, Liu T, et al. A positive feedback loop of AKR1C3-mediated activation of NF-kappa B and STAT3 facilitates proliferation and metastasis in hepatocellular carcinoma. Cancer Res 2021;81:1361-74.

66. Guo SS, Chen YZ, Liu LT, Liu RP, Liang YJ, Wen DX, et al. Prognostic significance of AKR1C4 and the advantage of combining EBV DNA to stratify patients at high risk of locoregional recurrence of nasopharyngeal carcinoma. BMC Cancer 2022;22:880.

67. Zhao SF, Wang SG, Zhao ZY, Li WL. AKR1C1-3, notably

AKR1C3, are distinct biomarkers for liver cancer diagnosis and prognosis: Database mining in malignancies. Oncol Lett 2019;18:4515-22.

68. Hu M, Sun D, Yu J, Fu Y, Qin Z, Huang B, et al. Brusatol sensitizes endometrial hyperplasia and cancer to progestin by suppressing NRF2-TET1-AKR1C1-mediated progestin metabolism. Lab Invest 2022;102:1335-45.

69. Li C, Tian ZN, Cai JP, Chen KX, Zhang B, Feng MY, et al. Panax ginseng polysaccharide induces apoptosis by targeting Twist/AKR1C2/NF-1 pathway in human gastric cancer. Carbohydr Polym 2014;102:103-9.

70. Xu Y, Qi W, Wang X, Zhang Y, Han L, Shi J, et al. Signal transducer and activator of transcription 3 cooperates with androgen receptor/cell cycle-related kinase signalling pathway in the progression of hepatitis B virus infection and gender differences. J Viral Hepat 2022;29:569-578.

71. Jin YX, Zhou XF, Chen YY, Jin WX, Wang YH, Ye DR, et al. Up-Regulated AKR1C2 is correlated with favorable prognosis in thyroid carcinoma. J Cancer 2019;10:3543-52.

72. Bremmer F, Jarry H, Unterkircher V, Kaulfuss S, Burfeind P, Radzun HJ, et al. Testosterone metabolites inhibit proliferation of castration- and therapy-resistant prostate

cancer. Oncotarget 2018;9:16951-61.

73. Sims AH, Howell A, Howell SJ, Clarke RB. Origins of breast cancer subtypes and therapeutic implications. Nat Clin Pract Oncol 2007;4:516-25.

74. Skibinski A, Kuperwasser C. The origin of breast tumor heterogeneity. Oncogene 2015;34:5309-16.

75. Yin L, Duan JJ, Bian XW, Yu SC. Triple-negative breast cancer molecular subtyping and treatment progress. Breast Cancer Res 2020;22:61.

76. Roswall P, Bocci M, Bartoschek M, Li H, Kristiansen G, Jansson S, et al. Microenvironmental control of breast cancer subtype elicited through paracrine platelet-derived growth factor-CC signaling. Nat Med 2018;24:463-73.

국문 초록

삼중 음성 유방암(TNBC) 환자는 다른 아형을 가진 환자에 비해 원격 전이 위험이 증가한다. 이 연구에서는 TNBC의 원격 전이와 관련된 유전자와 기본 메커니즘을 확인하는 것을 목표로 하고 TNBC 환자 31명에서 외과적으로 확보한 유방암 조직을 사용하여 환자 유래 이종이식(PDX) 모델을 확립하였다. 이 중 15명의 환자에서 원격 전이가 발생함. 전이가 있는 환자에서 높게 발현이 되는 전이 관련 후보 유전자는 RNA 시퀀싱을 진행하여 확인하였다. Aldo-keto reductase family 1 member C2 (AKR1C2) 가 유방암에서의 영향을 확인하기 위해 세포 활성, 세포 이동 능력 및 세포 침투 능력 측정 실험을 진행하였고 생체 내 실험을 진행하였고 종양 전이 분석을 수행하였다. 또한 METABRIC 데이터 세트를 사용하여 TNBC 하위 유형 및 다운스트림 신호 활동을 조절하는 AKR1C2의 잠재적 역할을 조사하였다. 결과 원발성 및 PDX 종양의 RNA 시퀀싱은 AKR1C2를 포함하여 스테로이드 호르몬 생합성에 관여하는 유전자가 이후에 전이가 발생한 환자에서 상당히 상향 조절되었음을 보여주었다. 시험관 내 및 생체 내 실험에서는 AKR1C2가 줄어들 경우 유방암 세포 증식, 이동, 침습, 종양 성장 및 폐 전이 발생률을 감소시키는 것으로 나타났다. AKR1C2는 METABRIC 데이터 세트에서 TNBC의 루미날 안드로겐 수용체(LAR) 하위 유형에서 상향 조절되었으며, AKR1C2의 억제는 TNBC 세포주에서 LAR 하위 유형 유전자의 하향 조절을 초래하였다. 안드로겐 수용체(AR) 유전자는 TNBC 세포에서 AKR1C2의 발현을 통해 조절되었다. AKR1C2의 발현은

JAK-STAT 신호 경로와 AR 발현을 조절하는 유전자 발현 경로와 관련이 있었다. AKR1C2가 억제된 TNBC 세포에서 phospho-signal transducer and activator of transcription (p-STAT3), IL-6의 발현 및 세포에서 분비된 IL-6는 모두 하향 조절되었다. 이러한 연구 결과는 AKR1C2가 TNBC에서 암의 성장 및 전이의 중요한 조절자이며 LAR 하위 유형 기능의 중요한 결정 요인일 수 있음을 나타낸다.

주요어: AKR1C2, 안드로겐 수용체, 삼중 음성 유방암, 종양 전이

학번: 2020-39163

Many thanks to the following people for their help with this study. Woochan Lee, Woohang Heo, Hye-Youn Son, Yujeong Her, Jong-Il Kim, and Hyeong-Gon Moon.